R. & M. No. 2747
(12,355, 14,166)
(A.R.C. Technical Report)

MINISTRY OF SUPPLY

AERONAUTICAL RESEARCH COUNCIL
REPORTS AND MEMORANDA

Model Tests on the Effects of Slipstream on the Flow at Various Tailplane Positions on a Four-Engined Aircraft

PART I

Tests with Contra-rotating Propellers

By
D. E. Hartley, B.A., A. Spence, B.Sc., and D. A. Kirby, B.Sc.

PART II

Tests with Single Rotating Propellers

By
D. A. Kirby, B.Sc.

LONDON: HER MAJESTY'S STATIONERY OFFICE
1955
TEN SHILLINGS NET

Model Tests on the Effects of Slipstream on the Flow at Various Tailplane Positions on a Four-Engined Aircraft

COMMUNICATED BY THE PRINCIPAL DIRECTOR OF SCIENTIFIC RESEARCH (AIR),
MINISTRY OF SUPPLY

*Reports and Memoranda No. 2747**
March, 1951

PART I

Tests with Contra-rotating Propellers

By
D. E. HARTLEY, B.A., A. SPENCE, B.Sc.,
and D. A. KIRBY, B.Sc.

Summary.—Systematic wind-tunnel tests have been made to investigate the effects of slipstream on the flow near the tailplane of a typical civil transport with four contra-rotating propellers. Tailplane height has been varied for each of several wing-body arrangements ; only one tailplane and one propeller position have been used. This report presents the main results in the form of changes in mean downwash angle, and velocity at the tailplane, as functions of tailplane position, lift coefficient, and propeller thrust. It is shown that the regions of increased downwash and velocity each extend for a range of tailplane height of about one propeller diameter whilst the region of increased downwash is displaced upwards a quarter of a diameter relative to the region of increased velocity.

A comparison of this work with flight results (R. & M. 2701[3]), in which the propellers were single rotating, show an apparent difference in the spread of the slipstream between single rotating and contra-rotating propellers.

1. *Introduction.*—With a view to improving existing methods for the prediction of longitudinal stability of civil aircraft, a series of model tests is being made in the Royal Aircraft Establishment No. 1, 11½ ft Wind Tunnel. One part of this is reported in Ref. 1 which deals with the effects of the fuselage. The present report describes tests on the effects of slipstream.

The major components of these effects are as follows :—

(*a*) increase of lift coefficient

(*b*) thrust moment

(*c*) change of wing pitching moment

(*d*) change of downwash at tailplane

(*e*) change of velocity at tailplane.

* R.A.E. Report Aero 2322, received 20th May, 1949.
R.A.E. Report Aero 2322a, received 23rd July, 1951.

This report deals with variations in the flow at the tailplane with tailplane height for a model which is typical of present-day propeller-turbine driven civil aircraft and has four contra-rotating propellers. Downwashes and velocities are deduced from force and moment measurements using the tailplane as an indicator of zero mean downwash and of comparative tail efficiency with and without slipstream. The overall force measurements are not applicable to full-scale because of the low Reynolds numbers of wing and tailplane, particularly the latter, and are not recorded. The changes in downwash and velocity at a given no-thrust lift coefficient should however be more reliable. Effects of slipstream on lift and pitching moment without tailplane are also recorded.

Attention is drawn to a recent collection[3], from flight tests of the movement of neutral point caused by slipstream on multi-engined aircraft with single rotating propellers.

2. *Model Details.*—The main dimensions of the model are given in Table 1 and illustrated in Figs. 1 to 3. The fuselage of Ref. 1 was used enabling changes of wing height, wing-body angle and tail arm to be made. The wing aspect ratio was 10 and the chord was made constant over the part of the wing behind the propellers. The section used was a modified R.A.F. 44, chosen to give as good characteristics as possible at the low Reynolds number ($0 \cdot 42 \times 10^6$) of the tests. Some turbulence was introduced into the tunnel by placing a fine-mesh honeycomb about four feet ahead of the model ; this in some respects gives lift and pitching-moment curves corresponding to a higher Reynolds number.

Six-bladed contra-rotating propellers were fitted in one typical position, 55 per cent root-chord ahead of the wing leading edge with the thrust line parallel to the wing chord and 5 per cent chord below it. The diameter chosen was one tenth of the wing span, and the spanwise positions were 22 per cent and 43 per cent of the semispan from the centre-line of the model. The propellers were driven by 3 h.p. electric motors which formed the main part of the nacelles.

Several alternative rear bodies could be fitted as shown in Fig. 2. The plan view was the same in all cases. Most of the tests were made with the deep knife-edged one which enabled a large number of tailplane heights to be used. Comparison has been made (section 4.3.2) of results for this body with those for the pointed rear bodies on each of which only one tailplane position was obtainable.

Split flaps of 20 per cent chord and 51 per cent semi-span per side, deflected at 60 deg, could be fitted as shown in Fig. 1. With a mid-wing, these were placed close to the fuselage ; for the low wing, the spanwise position was the same, leaving a gap equal to the diameter of the fuselage in the centre of the flap.

The tailplane setting was variable but the elevators, which were cut, were not used.

3. *Tests Made.*—The tests were made in the No. 1, $11\frac{1}{2} \times 8\frac{1}{2}$ ft Wind Tunnel at the R.A.E. between August and December, 1948. The wind speed was kept constant at 80 ft/sec to enable a range of thrust coefficient up to $0 \cdot 5$ to be used. This gave a Reynolds number of $0 \cdot 42 \times 10^6$.

Measurements were made of lift and pitching-moment coefficients with tailplane at two settings and without tailplane for lift coefficients up to about $0 \cdot 8$ (without slipstream) and for a range of thrust coefficient up to $0 \cdot 5$. This high value was chosen to exceed the most severe T_c against C_L relationship of the type of aircraft considered and also to give greater accuracy in the measurements.

The following table summarises the model configurations used ; those with flaps up are illustrated in Fig. 2.

Wing height	Wing-body angle (deg)	Tail arm $\div \bar{c}$	Rear body shape*	Tailplane height $\div$ propeller diameter	
				above fuselage centre-line	above wing root chord
(a) Flaps 0 deg					
Low	0	3·78	D	−0·15 0·00 +0·15 +0·30 +0·395	0·16 0·31 0·46 0·61 0·705
			P	0·00 +0·395	0·31 0·705
		4·41	D	−0·30 −0·15 +0·15 +0·30	0·01 0·16 0·46 0·61
			P	0·00 +0·395	0·31 0·705
	4	3·78	D	−0·20 0·00 +0·20	0·37 0·57 0·77
Mid	0	3·78	D	−0·15 +0·10	−0·15 +0·10
(b) Flaps 60 deg					
Low	0	3·78	D	−0·25 −0·15 +0·15	+0·06 0·16 0·46
Mid	0	3·78	D	+0·10 +0·30	0·10 0·30

* D is deep rear body,
P is pointed rear body.

In general the high thrust coefficients were used only at the two highest incidences. However, for four conditions as follows :—

(a) low wing, wing-body angle 0 deg, $l = 3 \cdot 78\bar{c}$, $Z_t/D = 0 \cdot 06$ and $0 \cdot 16$ and

(b) low wing, wing-body angle 4 deg, $l = 3 \cdot 78\bar{c}$, $Z_t/D = 0 \cdot 37$ and $0 \cdot 57$

tests were made at thrust coefficients of 0, 0·12 and 0·50 from zero lift up to $C_L = 0 \cdot 8$ in order to amplify the range of results.

4. *Results and Discussion.*—4.1. *Presentation.*—The results have been analysed to give the effects of propeller thrust on the mean downwash and mean velocity over the tailplane. The downwash angle was obtained by interpolating to find the tailplane setting for zero tailplane load ; the velocity has been expressed by the fractional increase b where

$$(V/V_0)^2 = (1 + b)^2 = \left(\frac{dC_m}{d\eta_T}\right) \div \left(\frac{dC_m}{d\eta_T} \text{ at zero thrust}\right) .$$

The increments $\Delta\varepsilon$ and b caused by thrust are given in Tables 4 to 9 and Figs. 8 to 16 at the end of the report.

For completeness the measurements of lift and pitching moment without tailplane are given in Tables 2 and 3 and Figs. 6a and 6b. The lift coefficients include the component of the thrust, but the thrust moment has been subtracted from the pitching-moment coefficients.

4.2 *Lift and Pitching-Moment Changes without Tailplane.*—The pitching-moment curves of Figs. 6a and 6b show that the change of moment caused by the thrust on the wing-body combination is small with flaps up but much more important with flaps down. In both cases the effect is stabilising. No satisfactory method of estimating the changes has been found.

The lift increments (excluding the thrust component) have been compared with estimates from R. & M. 1788[2] (Smelt and Davies). The comparison is made in Fig. 7 where the lift increment divided by the local lift coefficient without thrust is shown. In Smelt's form

$$\Delta C_L = \Delta C_{L\,(\mathrm{BOSS})} + (\lambda C_{L0} - 0\cdot 6 a_0\,\theta)\,\frac{D_1 c}{S}\,s$$

the predominating term is $\lambda C_{L0}/D_1 cs/S$ and the value for λ for the present model would be $1\cdot 8$ taking the aspect ratio of the part of the wing in the slipstream to include that covered by the fuselage. The experimental values of λ are $1\cdot 3$ for flaps up with all wing positions and for flaps down with mid wing ; for low wing with flaps down (with a central gap) the value of λ is $1\cdot 0$. Evidently the extra circulation caused by the thrust does not extend fully across the fuselage with flaps up, or on the mid-wing with flaps down ; and does not extend across at all for the low wing with flaps down because of the gap in the middle of the flap.

4.3 *Downwash and Velocity at Tailplane, Flaps Up.*—4.3.1. *With Deep Rear Body.*—It was expected that the mean increments of downwash and velocity would be functions of the height of the tailplane relative to the wing wake*. Following the collection of flight results (R. & M. 2701[3]), the angular parameter θ (defined in Fig. 4) was tried. The downwash changes with the longer tail arm, however, showed that for the present purpose the actual tailplane height or height in propeller diameters was a better parameter (Fig. 8). This implies that, for contra-rotating propellers, the slipstream effects do not spread with increase of distance downstream over a practical range of tail arm.

The results are plotted in Figs. 9 and 10 against Z_W the height of the tailplane above the wake centre-line (*see* Fig. 4). Separate curves are drawn for each incidence and approximate values of lift coefficient are given. The exact values can be found from Tables 4 to 7. At a given thrust, downwash and velocity curves show lateral shifts with incidence which are due to the upward displacement of the slipstream by the upwash ahead of the wing. The effects are removed by plotting against Z, the vertical distance of the tailplane above the trailing edge of the wing (*see* Fig. 4). This is done in Figs. 11 and 12. Evidently for the particular wing-propeller configuration and tail arm, the downward displacement of the slipstream behind the wing is equal to its upward displacement in front of the wing. For any other wing-propeller arrangement the appropriate parameter would be $Z_W - \alpha F$ where F is a function of propeller overhang, wing chord and inclination of thrust-line to wing chord. In Figs. 9 to 12 the heights have been made dimensionless by dividing by propeller diameter.

On Fig. 11 the curves for $T_c = 0\cdot 5$ were drawn first. These curves scaled in the ratio of the factor $a/(1 + a)$ where $1 + 2a = \sqrt{(1 + 8T_c/\pi)}$ were found to fit the experimental points for the lower thrust coefficients†.

---

* The position of the wake was estimated from Ref. 4 using values of lift coefficient at zero thrust.

† $a\phi/(1 + a)$ is the theoretical flow deflection behind an actuator disc at an angle ϕ to the main air stream.

Similarly the curves of Fig. 12 for b were constructed from that for $T_c = 0 \cdot 5$ by scaling by the expected factor, $2a$.

The main features shown by Figs. 11 and 12 are :—

(*a*) the regions of increased downwash and increased velocity each extend over a range of tailplane height of about one propeller diameter

(*b*) the peak downwash change occurs $0 \cdot 22$ diameters above the peak velocity change

(*c*) there is a large downwash change at zero lift

(*d*) the extra downwash at higher incidence is proportional to the lift coefficient without thrust (and hence to the slipstream lift increment)

(*e*) change of wing height or wing-body angle has no systematic effect on the results.

It is emphasised that the usefulness of the tailplane height relative to the wing trailing edge arises from the particular model geometry.

4.3.2. *Comparison with Results for Pointed Rear Bodies.*—The following table compares the values of $\Delta\varepsilon$ and b for the mid and high-pointed rear bodies with values taken from the curves of Figs. 11 and 12 for corresponding tailplane heights on the deep rear body.

Tailplane height	Tail arm	$\alpha = 5 \cdot 5$ deg				$\alpha = 7 \cdot 6$ deg			
		$T_c = 0 \cdot 37$		$T_c = 0 \cdot 50$		$T_c = 0 \cdot 37$		$T_c = 0 \cdot 50$	
		P	D	P	D	P	D	P	D
I Comparison of values of $\Delta\varepsilon$ (deg)									
Mid	3·78	1·25	1·55	1·7	1·9	0·9	1·0	1·45	1·25
Mid	4·41	1·05	1·15	1·5	1·4	0·55	0·4	0·9	0·5
High	3·78	0·80	1·2	1·1	1·45	1·3	1·95	1·7	2·4
High	4·41	1·05	1·45	1·5	1·7	1·7	2·4	2·15	2·9
II Comparison of values of b									
Mid	3·78	0·21	0·21	0·23	0·27	0·25	0·23	0·33	0·30
Mid	4·41	0·24	0·23	0·29	0·29	0·21	0·21	0·29	0·28
High	3·78	0·02	0·01	0·02	0·02	0·05	0·05	0·06	0·06
High	4·41	0·03	0·03	0·04	0·04	0·05	0·08	0·06	0·11

P is pointed rear body, D is deep rear body.

The velocity increments are in good agreement. The values of $\Delta\varepsilon$ agree for the mid-tail position, but for the high tail the downwash increments are smaller with the pointed rear body by about $0 \cdot 4$ deg at $\alpha = 5 \cdot 5$ deg and $0 \cdot 7$ deg at $\alpha = 7 \cdot 6$ deg. The curves of Fig. 11 may therefore overestimate the destabilising effects of slipstream for a high tailplane on an unswept pointed rear body.

4.4. *Downwash and Velocity at Tailplane, Flaps* 60 *deg.*—The increments of downwash and velocity with flaps at 60 deg are given in Table 8 for the model with low wing and Table 9 for mid-wing. Over the very limited range of tailplane position and incidence used, Figs. 13 to 16 show no systematic variations with incidence. Also, unlike the case with flaps up, the results are no more orderly when plotted against the height of the tailplane above the wing trailing edge than when plotted against the height above the wake. In Figs. 13 to 16, the factors $a/(1 + a)$(for $\Delta\varepsilon$) and $2a$ (for b) have been used to obtain the curves for low values of T_c from those for $T_c = 0 \cdot 5$.

The downwash changes for the mid-wing model are larger than those for the low wing. The larger lift increments caused by slipstream for the mid-wing (section 4.2) are not sufficient to account for the difference. It is not possible to suggest a reason from the scanty data available. The velocity changes are similar in the two cases.

The range of tailplane height used was not wide enough to define the positions or values of maximum $\Delta\varepsilon$ and b. Both $\Delta\varepsilon$ and b increase with decrease of tailplane height down to the lowest position used. Curves from the results with flaps up are shown on Figs. 13 to 16 in broken lines for purposes of comparison. The agreement between the results with flaps up and flaps down is best on the basis of tailplane height above the wake, but the variations with tailplane height are less rapid with flaps down.

5. *Concluding Remarks.*—The range of validity of the present results is limited for the following reasons :—

(*a*) only one position of the propellers was used

(*b*) only one tailplane span was tested

(*c*) the downwash increments caused by slipstream are smaller with an unswept pointed body than for a high tail position on the deep body

(*d*) the data with flaps deflected are very scanty.

With these limitations in mind, the investigation has shown that for contra-rotating propellers, the changes of downwash and velocity at the tailplane due to thrust each extend over a range of tailplane height of about one propeller diameter, the peak downwash change occurring 0·22 diameters higher than the peak velocity. For a given tailplane position and incidence, the variations with thrust coefficient are given by

$$\Delta\varepsilon \propto a/(1 + a)$$

$$b \propto a$$

where

$$1 + 2a = \sqrt{(1 + 8T_c/\pi)}.$$

In order to make the results more generally applicable, tests would be required on different tailplane spans and propeller positions. Further work would also be needed on lift and pitching-moment changes without tailplane, particularly with flaps deflected, and the present limited range of results with flaps would require extending.

Certain differences are apparent between the flight results (R. & M. 2701[3]) in which the propellers were single rotating, and these model tests on contra-rotating propellers ; in particular the slipstreams appear to spread in different manners. In order to investigate these differences some of the tests have been repeated using single rotating propellers (Part II).

PART II

Tests with Single Rotating Propellers

By

D. A. KIRBY, B.Sc.

Summary.—This part of the report gives the results of tests which have been made on the model of Part I fitted with single rotating propellers.

(*a*) As with contra-rotating propellers the region of increased downwash due to slipstream is displaced upwards a quarter of a propeller diameter relative to the region of increased velocity.

(*b*) Unlike the contra-rotating propellers, there is evidence of some spread in the slipstream proportional to the tail arm. The variation of downwash increment with incidence was less than that obtained with the contra-rotating propellers.

These conclusions imply that the destabilising effect is smaller than for contra-rotating propellers. For the range of tail arm considered, the difference in slipstream spread would not have much effect on the variation of the destabilising effect with tailplane height. The difference in slipstream spread is not sufficient to explain differences from flight results (R. & M. 2701[3]).

---

1. *Introduction.*—Comparison of the results of Part I with flight results (R. & M. 2701[3]) in which the propellers were single rotating suggests certain differences; in particular the slipstreams appear to spread in different manners. To extend the previous work tests have been made with single rotating propellers. Downwashes and velocities were deduced from force and moment measurements as in Part I.

The previous tests showed that the same position of the tailplane relative to the slipstream wake could be obtained with several different wing and body arrangements without affecting the values of the increments of downwash and velocity due to thrust. The tests with single rotating propellers have been made with only one arrangement—a low wing with a geometric wing-body angle of 0 deg.

2. *Model Details.*—The model used was that of Part I with the six-bladed contra-rotating propellers replaced by three-bladed single rotating propellers. The overhang of the propellers was 55 per cent root chord *i.e.*, midway between the front and rear components of the contra-rotating propellers. The deep rear body was used, but no tests were made with pointed rear bodies. Flaps were not fitted.

Relevant details of the model are given in Table 1 and the nacelle is illustrated in Fig. 17. The general arrangement of the model is shown in Fig. 1.

3. *Tests Made.*—The tests were made in the No. 1, $11\frac{1}{2}$ ft $\times$ $8\frac{1}{2}$ ft Wind Tunnel at the R.A.E. during October, 1950. The test conditions were the same as those of Part I, the fine-mesh honeycomb being placed ahead of the model and the wing speed being 80 ft/sec (Reynolds number $0 \cdot 42 \times 10^6$).

Measurements were made of lift and pitching-moment coefficients with the tailplane at two settings and without tailplane, for lift coefficients up to about 0·8 (without slipstream), and for thrust coefficients of 0, 0·37 and 0·50. The following table summarises the model conditions used.

Tail arm $\div \bar{c}$	Tailplane height $\div$ propeller diameter	
	above fuselage centre-line	above wing root chord
3·78	No tailplane	
	−0·15	0·16
	0·00	0·31
	0·15	0·46
	0·30	0·61
4·41	No tailplane	
	0·15	0·46
	0·30	0·61

4. *Results and Discussion.*—4.1. *Presentation.*—The effects of propeller thrust on the mean downwash and mean velocity over the tailplane have been calculated as in Part I. The increments $\Delta\varepsilon$ and b caused by thrust are given in Tables 11 and 12 and Figs. 21 to 25 at the end of the report.

The measurements of the lift and pitching moment without tailplane are given in Table 10. The lift coefficients include the component of the thrust, but the thrust moment has been subtracted from the pitching-moment coefficients.

4.2. *Lift and Pitching-Moment Changes without Tailplane.*—A comparison of Fig. 19 with Fig. 6 shows that the change of pitching moment caused by the thrust on the wing and body is rather larger (*i.e.*, more stabilising) with single rotating propellers than with contra-rotating propellers.

Fig. 20 shows the lift increments (excluding the thrust component) as measured with the single rotating propellers, and compares them with the results for the contra-rotating propellers and also with calculated values[2]. It is seen that the single and contra-rotating propeller results are in fair agreement, both being less than the calculated values.

4.3. *Downwash and Velocity at Tailplane.*—For contra-rotating propellers the flow pattern changes only slowly with distance downstream, because there is little or no rotation in the flow. In Part I it was shown that the effects on downwash and velocity for tail arms of $3 \cdot 78\bar{c}$ and $4 \cdot 41\bar{c}$ fitted on the same curves against the parameter Z_W/D, where Z_W is the height of the tailplane above the wing wake (calculated from Ref. 4 for the lift at zero thrust). The effects were confined to regions about one propeller diameter in depth.

With single rotating propellers, passing over the wing will remove the primary rotation in the flow but local rotations remain and the effects of the slipstream would be expected to spread and to be dissipated more quickly than with contra-rotating propellers. The downwash increments are plotted against Z_W/D in Fig 21 which shows that the peak downwash is smaller and the spread greater for the longer tail arm. Fig. 22 illustrates that the results for the two tail arms lie on the same curves if $\Delta\varepsilon \times l/\bar{c}$ is plotted against $(Z_W/D) \div (l/\bar{c})$, i.e., the spread is assumed to vary as the tail arm. Downwash increments for single and contra-rotating propellers are compared in Fig. 23 on a scale of Z_W/D. The results are fairly similar in the middle of the incidence range, but with single rotating propellers the effect of incidence is only about half as large as for contra-rotating propellers with the shorter tail arm and would be still less with the longer tail arm.

The velocity increments are shown in Fig. 24. There is no decrease with increase of tail arm, probably because the slipstream spreads further into the region near the side of the body and the increase in the proportion of tailplane span affected offsets the reduction in local velocity. There is some evidence of larger spread at the longer tail arm and there is slightly better agreement between the two tail arms when the increments are plotted against $(Z_W/D) \div (l/\bar{c})$ as in Fig. 25

The results also show that :—

(*a*) for the shorter tail arm the peaks of the downwash and velocity increments are separated by about 0·22 propeller diameters, the same as for contra-rotating propellers. There is not enough data to check that this is also true for the longer tail arm

(*b*) the values of $\Delta\varepsilon$ at $T_c = 0{\cdot}37$ are 10 per cent less than would be obtained by scaling from $T_c = 0{\cdot}5$ assuming $\Delta\varepsilon$ proportional to $a/(1 + a)$ as in Part I ; the values of b are proportional to a where $1 + 2a = \sqrt{(1 + 8T_c/\pi)}$.

Combining the greater stabilising effect on the wing-body unit with the smaller variation of $\Delta\varepsilon$ as incidence increases for the single rotating propellers, the overall destabilising effect is smaller than for contra-rotating propellers. For the range of tail arm considered, the difference in slipstream spread would not have much effect on the variation of the destabilising effect with tailplane height.

LIST OF SYMBOLS

(*a*) *General*

C_{L0}	Lift coefficient at zero thrust, no tailplane
C'_{L0}	Local value of C_{L0} across flapped part of wing
l	Tail arm (wing quarter-chord to tailplane quarter-chord)
ε	Mean downwash angle at tailplane
$\Delta\varepsilon$	Change of ε from value at zero thrust
b	Fractional increase of mean velocity at tailplane defined by $(1 + b)^2 = \frac{dC_m}{d\eta_T} \div \left(\frac{dC_m}{d\eta_T} \text{ at zero thrust}\right)$

(*b*) *Propellers*

D	Propeller diameter
T_c	Thrust coefficient (thrust $\div \rho V^2 D^2$)
a	Defined by $1 + 2a = \sqrt{(1 + 8T_c/\pi)}$

(*c*) *Tailplane height* (*see* Fig. 4)

Z_t	Height of tailplane quarter-chord above wing root chord
Z_W	Height of tailplane quarter-chord above wing wake
Z	Height of tailplane quarter-chord above wing trailing edge at root measured perpendicular to main stream
θ	Angular height of tailplane leading edge above line joining wing root trailing edge to position of wake below elevator hinge-line (definition as used in R. & M. 2701[3]).

REFERENCES

No.	Author		Title, etc.
1	A. Anscombe and D. J. Raney	..	Low-speed tunnel investigation of the effect of body on C_{m0} and aerodynamic centre of unswept wing-body combinations. C.P.16. April, 1949.
2	R. Smelt and H. Davies ..	..	Estimation of the increase in lift due to slipstream. R. & M. 1788. December, 1936.
3	D. E. Morris and J. C. Morall ..	..	The effect of slipstream on the longitudinal stability of multi-engined aircraft. R. & M. 2701. November, 1948.
4	A. Silverstein and S. Katzoff ..	..	Design charts for predicting downwash angles and wake characteristics behind plain and flapped wings. N.A.C.A. Report 648. 1939. (A.R.C. 3981.)

TABLE 1

Details of Model

Wing		
Span	100 in.	
Mean chord	9·97 in.	
Root chord	11·07 in.	
Gross area	6·92 sq ft	
Aspect ratio	10	
Dihedral	None except on lower surfaces of outboard sections	
Section	RAF44 Modified to have straight portion from 65·5 per cent chord to trailing edge on upper surface. Maximum thickness ratio 15 per cent at 30 per cent chord; camber 2·4 per cent $\bar{c}$ at 30 per cent $\bar{c}$.	
Body		
Overall lengths (i)	68·3 in.	
(ii)	74·6 in.	
Diameter	9 in.	
Tailplane		
Span	32 in.	
Mean chord	6·16 in.	
Gross area	1·37 sq ft	
Aspect ratio	5·2	
Tail arms (i)	37·64 in. (3·78$\bar{c}$)	
(ii)	43·94 in. (4·41$\bar{c}$)	
Tail volume ratios (i)	0·75	
(ii)	0·90	
Airscrews		
Type	Contra-rotating	Single rotating
Number of blades each	6	3
Diameter	10 in.	10 in.
Solidity	0·24	0·12
Blade angle at 0·7 radius	35 deg	30 deg
Distance forward of wing leading edge	6·16 in.	6·16 in.
Flaps		
Type	Split	
Span (per side)	25·5 in.	
Inner edge from model centre-line	4·5 in.	
Chord	2·2 in.	
Deflection	60 deg	
Distance of hinge from trailing edge at wing root	2·2 in.	
Pitching-moment axis		
Distance aft of leading edge at wing root	2·77 in.	
Distance below chord-line	0·67 in.	
Distance aft of leading-edge standard mean chord	0·25$\bar{c}$	

TABLE 2

Lift and Pitching-Moment Coefficients without Tailplane. Deep Rear Body

Contra-rotating Propellers

(a) Low wing
Wing-body angle 0 deg
$l = 3 \cdot 78\bar{c}$

α	T_c	C_L	C_L Trim	C_m
−0·80	0	0·028	0·019	−0·0330
+0·25	0	0·124	0·120	−0·0153
1·30	0	0·209	0·209	−0·0019
	0·12	0·226	0·225	−0·0050
3·40	0	0·388	0·397	+0·0302
	0·12	0·423	0·432	0·0344
	0·25	0·451	0·457	0·0242
5·50	0	0·589	0·604	0·0512
	0·12	0·653	0·667	0·0524
	0·25	0·692	0·705	0·0481
	0·37	0·727	0·739	0·0456
	0·50	0·763	0·774	0·0416
7·60	0	0·800	0·821	0·0795
	0·12	0·871	0·893	0·0825
	0·25	0·923	0·946	0·0860
	0·37	0·977	0·988	0·0783
	0·50	1·029	1·049	0·0740
+9·65	0	0·940	0·967	+0·1031

(b) Low wing
Wing-body angle 0 deg
$l = 4 \cdot 41\bar{c}$

α	T_c	C_L	C_L Trim	C_m
−0·80	0	0·040	0·032	−0·0339
+0·25	0	0·129	0·125	−0·0170
1·30	0	0·216	0·216	−0·0003
	0·12	0·235	0·234	−0·0029
3·40	0	0·406	0·413	+0·0286
	0·12	0·447	0·453	0·0279
	0·25	0·473	0·478	0·0229
5·50	0	0·606	0·618	0·0534
	0·12	0·675	0·687	0·0541
	0·25	0·714	0·725	0·0496
	0·37	0·750	0·760	0·0442
	0·50	0·787	0·796	0·0399
7·60	0	0·804	0·822	0·0803
	0·12	0·881	0·900	0·0826
	0·25	0·938	0·956	0·0795
	0·37	0·986	1·003	0·0737
	0·50	1·040	1·056	0·0699
+8·65	0	0·885	0·906	+0·0936

Note : C_L includes component of propeller thrust
C_m excludes the moment of the thrust

(c) Mid Wing
Wing-body angle 0 deg
$l = 3 \cdot 78\bar{c}$

α	T_c	C_L	C_L Trim	C_m
−0·80	0	0·052	0·043	−0·0324
+0·25	0	0·154	0·149	−0·0191
1·30	0	0·226	0·224	−0·0070
	0·12	0·240	0·238	−0·0084
3·40	0	0·401	0·409	+0·0313
	0·12	0·438	0·446	0·0315
	0·25	0·468	0·475	0·0274
5·50	0	0·615	0·630	0·0553
	0·12	0·679	0·694	0·0567
	0·25	0·725	0·737	0·0524
	0·37	0·764	0·777	0·0502
	0·50	0·804	0·816	0·0467
7·60	0	0·816	0·840	0·0826
	0·12	0·890	0·912	0·0845
	0·25	0·952	0·974	0·0812
	0·37	1·000	1·020	0·0769
	0·50	1·060	1·080	0·0744
+8·65	0	0·888	0·914	+0·0998

(d) Low wing
Wing-body angle 4 deg
$l = 3 \cdot 78\bar{c}$

α	T_c	C_L	C_L Trim	C_m
−0·80	0	0·014	−0·006	−0·0745
+0·25	0	0·097	+0·082	−0·0567
1·30	0	0·178	0·168	−0·0392
	0·12	0·189	0·178	−0·0429
3·40	0	0·362	0·359	−0·0102
	0·12	0·398	0·396	−0·0104
	0·25	0·418	0·414	−0·0134
5·50	0	0·558	0·563	+0·0204
	0·12	0·620	0·626	0·0226
	0·25	0·660	0·665	0·0203
	0·37	0·687	0·692	0·0177
	0·50	0·727	0·731	0·0135
7·60	0	0·760	0·772	0·0451
	0·12	0·823	0·836	0·0497
	0·25	0·883	0·896	0·0484
	0·37	0·927	0·939	0·0471
	0·50	0·967	0·979	0·0441
+8·60	0	0·844	+0·859	+0·0571

TABLE 2—*continued*

(e) Low wing
Wing-body angle 0 deg
$l = 3\cdot78\bar{c}$

α	T_c	C_L	C_L Trim	C_m
−1·30	0	+0·002	−0·008	−0·0398
	0·12	−0·009	−0·022	−0·0480
	0·50	−0·026	−0·043	−0·0649
+1·30	0	+0·226	0·226	−0·0016
	0·12	0·242	0·241	−0·0046
	0·50	0·274	0·269	−0·0191
3·40	0	0·400	0·406	+0·0241
	0·12	0·443	0·449	0·0237
	0·50	0·512	0·515	0·0117
+5·50	0	0·605	0·618	0·0497
	0·12	0·666	0·679	0·0506
	0·50	+0·775	0·786	+0·0413

(f) Low wing
Wing-body angle 4 deg
$l = 3\cdot78\bar{c}$

α	T_c	C_L	C_L Trim	C_m
−1·30	0	−0·003	−0·023	−0·0749
	0·12	−0·018	−0·040	−0·0822
	0·50	−0·033	−0·058	−0·0958
+1·30	0	+0·205	+0·194	−0·0407
	0·12	0·218	0·207	−0·0430
	0·50	0·249	0·235	−0·0523
3·40	0	0·381	0·378	−0·0114
	0·12	0·422	0·419	−0·0103
	0·50	0·487	0·482	−0·0176
+5·50	0	0·576	0·581	+0·0183
	0·12	0·632	0·637	0·0204
	0·50	+0·729	+0·733	+0·0165

TABLE 3

Lift and Pitching-Moment Coefficients without Tailplane. Deep Rear Body

Contra-rotating Propellers

(a) Low wing
Flaps down
Wing-body angle 0 deg
$l = 3\cdot78\bar{c}$

α	T_c	C_L	C_L Trim	C_m
1·65	0	0·978	0·967	−0·1180
	0·12	1·092	1·056	−0·1352
	0·25	1·173	1·135	−0·1544
	0·37	1·232	1·187	−0·1712
	0·50	1·293	1·254	−0·1841
3·75	0	1·160	1·135	−0·0934
	0·12	1·280	1·251	−0·1092
	0·25	1·382	1·347	−0·1306
	0·37	1·443	1·404	−0·1460
	0·50	1·495	1·443	−0·1589
5·85	0	1·352	1·333	−0·0734
	0·12	1·473	1·451	−0·0842
	0·25	1·587	1·559	−0·1047
	0·37	1·654	1·623	−0·1184
	0·50	1·731	1·696	−0·1312
7·95	0	1·549	1·536	−0·0494
	0·12	1·678	1·662	−0·0623
	0·25	1·789	1·769	−0·0766
	0·37	1·870	1·846	−0·0904
	0·50	1·950	1·923	−0·1016

(b) Mid-wing
Flaps down
Wing-body angle 0 deg
$l = 3\cdot78\bar{c}$

α	T_c	C_L	C_L Trim	C_m
−5·70	0	0·259	0·203	−0·2102
−3·60	0	0·456	0·409	−0·1768
	0·12	0·538	0·481	−0·2150
−1·50	0	0·652	0·612	−0·1519
	0·12	0·747	0·698	−0·1849
	0·25	0·829	0·772	−0·2147
+0·60	0	0·870	0·835	−0·1330
	0·12	0·973	0·930	−0·1631
	0·25	1·063	1·013	−0·1873
	0·37	1·147	1·092	−0·2079
	0·50	1·205	1·143	−0·2350
2·70	0	1·067	1·037	−0·1136
	0·12	1·205	1·168	−0·1408
	0·25	1·291	1·248	−0·1639
	0·37	1·360	1·312	−0·1815
	0·50	1·444	1·391	−0·1997
+3·80	0	1·157	1·130	−0·1009

TABLE 4

Effect of Slipstream on Mean Downwash and Velocity at Tailplane

Contra-rotating Propellers

Low wing — Wing-body angle 0 deg, Deep rear body — $l = 3 \cdot 78\bar{c}$

(a) ε at $T_c = 0$

α	C_L Trim	Z_t/D				
		0·16	0·31	0·46	0·61	0·705
−0·80	0·019	−1·00	0·35	0·35	1·55	2·30
+1·30	0·209	−0·40	1·20	1·10	1·90	2·55
3·40	0·397	+0·50	1·65	2·05	2·70	3·40
5·50	0·604	1·30	2·70	2·70	3·30	3·85
+7·60	0·821	+1·80	3·50	3·55	3·90	4·20

(b) Z_W

α	Z_t/D					
	0·06	0·16	0·31	0·46	0·61	0·705
−1·30	+0·124	0·224	0·374	0·524	0·674	0·769
−0·80	+0·107	0·206	0·358	0·506	0·658	0·752
+1·30	+0·042	0·140	0·292	0·441	0·593	0·686
3·40	−0·025	0·074	0·225	0·374	0·525	0·619
5·50	−0·086	0·013	0·164	0·312	0·462	0·556
+7·60	−0·145	−0·047	0·104	0·247	0·401	0·494

(c) Z/D

α	Z_t/D					
	0·06	0·16	0·31	0·46	0·61	0·705
−1·30	+0·126	+0·226	0·376	0·526	0·676	0·771
−0·80	+0·101	+0·200	0·352	0·500	0·652	0·746
1·30	−0·006	+0·092	0·244	0·393	0·545	0·638
3·40	−0·114	−0·015	0·136	0·285	0·436	0·530
5·50	−0·222	−0·123	0·028	0·176	0·326	0·420
7·60	−0·329	−0·231	−0·080	0·063	0·217	0·310

TABLE 4—*continued*

(d) $\Delta\varepsilon$

α	C_L Trim	Z_t/D 0·06	0·16	0·31	0·46	0·61	0·705	T_c
−1·3	−0·034	0·50	+0·45					
+1·3	0·225	0·35	0·35	0·45	0·25	0·15	0·20	
3·4	0·432	0·05	0·32	0·55	0·60	0·40	0·25	0·12
5·5	0·667	0·15	+0·12	0·40	0·95	0·70	0·50	
+7·6	0·893		−0·10	0·20	0·75	1·00	0·60	
3·4	0·457		0·70	1·05	1·10	0·70	0·55	
5·5	0·705		0·25	0·95	1·70	1·25	0·95	0·25
7·6	0·946		0·05	0·45	1·40	1·70	1·05	
5·5	0·739		0·30	1·40	2·25	1·65	1·25	
7·6	0·988		0·25	0·90	2·10	2·40	1·70	0·37
−1·3	−0·055	1·40	1·40					
+1·3	0·255	1·20	1·50					
3·4	0·501	0·45	0·90					0·50
5·5	0·774	0·50	0·60	1·85	2·90	2·15	1·60	
+7·6	1·049		0·25	1·45	2·75	3·05	2·40	

(e) b

α	C_L Trim	Z_t/D 0·06	0·16	0·31	0·46	0·61	0·705	T_c
−1·3	−0·034	0·055	0·005					
+1·3	+0·225	0·080	0·060	0·039	0·003	0·000	0·000	
3·4	0·432	0·097	0·084	0·086	0·028	0·000	0·000	0·12
5·5	0·667	0·070	0·047	0·080	0·050	0·004	0·000	
+7·6	+0·893		0·050	0·084	0·080	0·029	0·015	
3·4	0·457		0·160	0·128	0·035	0·011	0·000	
5·5	0·705		0·116	0·170	0·082	0·014	0·000	0·25
7·6	0·946		0·124	0·172	0·150	0·043	0·031	
5·5	0·739		0·170	0·230	0·100	0·026	0·000	
7·6	0·988		0·164	0·247	0·178	0·073	0·025	0·37
−1·3	−0·055	0·174	0·120					
+1·3	+0·255	0·252	0·240					
3·4	0·501	0·273	0·275					0·50
5·5	0·774	0·223	0·252	0·310	0·107	0·031	0·000	
+7·6	+1·049		0·208	0·336	0·241	0·104	0·020	

TABLE 5

Effects of Slipstream on Mean Downwash and Velocity at Tailplane

Contra-rotating Propellers

Low wing

Wing-body angle 0 deg
Deep rear body

$l = 4 \cdot 41\bar{c}$

(a) ε at $T_c = 0$

α	C_L Trim	Z_t/D			
		0·01	0·16	0·46	0·61
−0·8	0·032	−1·10	−0·20	0·40	1·30
+1·3	0·216	−0·30	−0·20	1·20	2·00
3·4	0·413	+0·30	+0·90	1·90	2·60
5·6	0·618	1·10	1·90	2·60	3·45
+7·7	0·822	+1·90	+2·40	3·15	4·40

(b) Z_W/D

α	Z_t/D			
	0·01	0·16	0·46	0·61
−0·8	+0·070	+0·223	0·521	0·670
+1·3	−0·009	+0·144	0·442	0·592
3·4	−0·081	+0·069	0·367	0·516
5·6	−0·157	−0·006	0·291	0·442
+7·7	−0·227	−0·077	0·218	0·367

(c) Z/D

α	Z_t/D			
	0·01	0·16	0·46	0·61
−0·8	0·059	+0·212	+0·510	0·659
+1·3	−0·072	+0·081	+0·379	0·529
3·4	−0·202	−0·050	+0·248	0·397
5·6	−0·332	−0·181	+0·116	0·267
+7·7	−0·461	−0·311	−0·016	0·133

(d) $\Delta\varepsilon$

α	C_L Trim	Z_t/D			
		0·01	0·16	0·46	0·61
1·3	0·234	+0·10	0·35	0·35	0·10
3·4	0·453	0·0	0·30	0·85	0·60
5·6	0·687	0·0	0·20	0·90	0·90
7·7	0·900	−0·20	−0·20	0·60	1·10
3·4	0·478	0·0	0·45	1·55	0·95
5·6	0·725	0·0	−0·05	1·55	1·40
7·7	0·956	−0·10	−0·20	1·35	1·95
5·6	0·760	0·0	−0·05	2·05	1·90
7·7	1·003	−0·10	−0·05	1·90	2·55
5·6	0·796	0·0	0·45	2·45	2·45
7·7	1·056	−0·10	−0·05	2·60	3·15

(e) b

Z_t/D				T_c
0·01	0·16	0·46	0·61	
0·044	0·070	0·015	0	0·12
0·034	0·100	0·020	0	
0·046	0·060	0·080	0	
0·025	0·020	0·095	0·070	
0·102	0·180	0·020	0	0·25
0·095	0·170	0·130	0	
0·063	0·070	0·200	0·115	
0·151	0·210	0·160	0	0·37
0·102	0·120	0·245	0·140	
0·204	0·310	0·135	0	0·50
0·155	0·145	0·285	0·140	

TABLE 6

Effects of Slipstream on Mean Downwash and Velocity at Tailplane

Contra-rotating Propellers

Mid-wing | Wing-body angle 0 | $l = 3 \cdot 78\bar{c}$

Deep rear body

(a) ε at $T_c = 0$ deg

α	C_L Trim	Z_t/D	
		$-0 \cdot 15$	$0 \cdot 10$
$-0 \cdot 8$	$0 \cdot 043$	$-0 \cdot 10$	$0 \cdot 00$
$+1 \cdot 3$	$0 \cdot 224$	$+0 \cdot 70$	$1 \cdot 30$
$3 \cdot 4$	$0 \cdot 409$	$1 \cdot 10$	$2 \cdot 10$
$5 \cdot 5$	$0 \cdot 630$	$1 \cdot 50$	$3 \cdot 20$
$+7 \cdot 6$	$0 \cdot 840$	$+1 \cdot 60$	$3 \cdot 90$

(b) Z_W/D

α	Z_t/D	
	$-0 \cdot 15$	$0 \cdot 10$
$-0 \cdot 8$	$-0 \cdot 099$	$+0 \cdot 152$
$+1 \cdot 3$	$-0 \cdot 166$	$+0 \cdot 085$
$3 \cdot 4$	$-0 \cdot 232$	$+0 \cdot 019$
$5 \cdot 5$	$-0 \cdot 291$	$-0 \cdot 042$
$+7 \cdot 6$	$-0 \cdot 350$	$-0 \cdot 101$

(c) Z/D

Z_t/D	
$-0 \cdot 15$	$0 \cdot 10$
$-0 \cdot 110$	$+0 \cdot 141$
$-0 \cdot 218$	$+0 \cdot 033$
$-0 \cdot 325$	$-0 \cdot 074$
$-0 \cdot 431$	$-0 \cdot 182$
$-0 \cdot 538$	$-0 \cdot 289$

(d) $\Delta\varepsilon$

α	C_L Trim	Z_t/D	
		$-0 \cdot 15$	$0 \cdot 10$
$1 \cdot 3$	$0 \cdot 238$	$0 \cdot 00$	$0 \cdot 30$
$3 \cdot 4$	$0 \cdot 446$	$0 \cdot 00$	$0 \cdot 20$
$5 \cdot 5$	$0 \cdot 694$	$-0 \cdot 10$	$-0 \cdot 05$
$7 \cdot 6$	$0 \cdot 912$	$0 \cdot 00$	$-0 \cdot 20$
$3 \cdot 4$	$0 \cdot 475$	$-0 \cdot 20$	$0 \cdot 50$
$5 \cdot 5$	$0 \cdot 737$	$-0 \cdot 20$	$0 \cdot 00$
$7 \cdot 6$	$0 \cdot 974$	$0 \cdot 00$	$-0 \cdot 10$
$5 \cdot 5$	$0 \cdot 777$	$-0 \cdot 20$	$0 \cdot 15$
$7 \cdot 6$	$1 \cdot 020$	$0 \cdot 00$	$0 \cdot 10$
$5 \cdot 5$	$0 \cdot 816$	$-0 \cdot 20$	$0 \cdot 30$
$7 \cdot 6$	$1 \cdot 080$	$0 \cdot 00$	$0 \cdot 40$

(e) b

Z_t/D		T_c
$-0 \cdot 15$	$0 \cdot 10$	
$0 \cdot 050$	$0 \cdot 081$	
$0 \cdot 050$	$0 \cdot 110$	$0 \cdot 12$
$0 \cdot 042$	$0 \cdot 081$	
$0 \cdot 019$	$0 \cdot 065$	
$0 \cdot 085$	$0 \cdot 186$	
$0 \cdot 074$	$0 \cdot 158$	$0 \cdot 25$
$0 \cdot 036$	$0 \cdot 130$	
$0 \cdot 100$	$0 \cdot 221$	
$0 \cdot 065$	$0 \cdot 193$	$0 \cdot 37$
$0 \cdot 145$	$0 \cdot 280$	
$0 \cdot 081$	$0 \cdot 202$	$0 \cdot 50$

TABLE 7

Effects of Slipstream on Mean Downwash and Velocity at Tailplane

Contra-rotating Propellers

Low wing — Wing-body angle 4 deg, Deep rear body — $l = 3 \cdot 78\bar{c}$

(a) ε at $T_C = 0$

α	C_L Trim	Z_t/D 0·37	0·57	0·77
−0·8	−0·006	−1·60	−0·40	0·20
+1·3	0·168	−0·80	+0·05	0·80
3·4	0·359	+0·00	0·48	1·60
5·5	0·563	0·75	1·10	2·15
+7·6	0·772	+1·90	+2·00	3·10

(b) Z_W/D

α	Z_t/D 0·37	0·57	0·77
−1·3	0·434	0·633	0·831
−0·8	0·418	0·618	0·817
+1·3	0·348	0·548	0·750
3·4	0·282	0·481	0·679
5·5	0·218	0·418	0·616
+7·6	0·156	0·354	0·552

(c) Z/D

Z_t/D 0·37	0·57	0·77
+0·437	0·636	0·834
0·415	0·615	0·814
0·307	0·507	0·709
0·199	0·398	0·596
+0·090	0·290	0·488
−0·018	0·180	0·378

(d) $\Delta\varepsilon$

α	C_L Trim	Z_t/D 0·37	0·57	0·77
−1·3	−0·040	0·20	0·1	—
+1·3	+0·178	0·45	0·35	0·15
3·4	0·396	0·55	0·60	0·30
5·5	0·626	0·55	1·0	0·45
+7·6	+0·836	0·45	0·8	0·60
3·4	0·414	1·00	0·98	0·40
5·5	0·665	1·15	1·50	0·75
7·6	0·896	0·85	1·60	1·10
5·5	0·692	1·55	1·9	0·95
7·6	0·939	1·30	2·2	1·40
−1·3	−0·058	0·90	0·40	—
+1·3	+0·235	1·60	0·85	—
3·4	0·482	2·00	1·6	—
5·5	0·731	1·95	2·35	1·25
+7·6	+0·979	1·70	2·80	1·80

(e) b

Z_t/D 0·37	0·57	0·77	T_c
0·005	0·000	—	0·12
0·025	0·000	0·0	
0·065	0·000	0·0	
0·080	0·025	0·0	
0·090	0·065	0·0	
0·095	0·00	0·0	0·25
0·13	0·05	0·00	
0·155	0·09	0·02	
0·170	0·06	0·0	0·37
0·215	0·111	0·03	
0·035	0·00	—	0·50
0·070	0·00	—	
0·130	0·03	—	
0·220	0·06	0·00	
0·260	0·11	0·04	

TABLE 8

Effects of Slipstream on Mean Downwash and Velocity at Tailplane

Contra-rotating Propellers

Low wing with flaps down — Wing-body angle 0 deg; Deep rear body — $l = 3 \cdot 78\bar{c}$

(a) ε at $T_c = 0$

α	C_L Trim	Z_t/D		
		0·06	0·16	0·46
−2·55	0·513	1·75	2·20	—
−0·45	0·727	2·25	2·70	3·60
+1·65	0·967	2·75	3·10	4·45
3·75	1·135	3·75	3·90	5·20
5·85	1·333		5·10	6·15
+7·95	1·536		5·85	6·85

(b) Z_W/D

α	Z_t/D		
	0·06	0·16	0·46
−2·55	0·648	0·745	1·045
−0·45	0·587	0·685	0·985
+1·65	0·529	0·626	0·926
3·75	0·472	0·569	0·869
5·85	0·400	0·500	0·800
+7·95	0·300	0·400	0·700

(c) Z/D

Z_t/D		
0·06	0·16	0·46
+0·192	+0·289	0·589
+0·084	+0·182	0·482
−0·023	+0·074	0·374
−0·130	−0·033	0·267
−0·240	−0·140	0·160
−0·348	−0·248	0·052

(d) $\Delta\varepsilon$

α	C_L Trim	Z_t/D		
		0·06	0·16	0·46
−2·55	0·587	0·80	0·30	
−0·45	0·823	0·50	0·55	
+1·65	1·056	0·90	0·60	0·15
3·75	1·251	0·90	0·80	0·45
5·85	1·451		0·55	0·30
+7·95	1·662		0·60	0·60
−0·45	0·892	1·10	0·65	
+1·65	1·135	1·15	1·05	
3·75	1·347	1·50	1·25	0·80
5·85	1·559		1·25	0·70
+7·95	1·769		1·25	0·95
1·65	1·187	1·65	1·20	
3·75	1·404	1·85	1·65	
5·85	1·623		1·45	0·90
7·95	1·846		1·80	1·15
1·65	1·254	1·70	1·50	
3·75	1·443	2·10	1·95	
5·85	1·696		1·55	1·00
7·95	1·923		1·85	1·40

(e) b

Z_t/D			T_c
0·06	0·16	0·46	
0	0·010		
0	0·010		
0·010	0·010	0	
0·030	0·030	0	0·12
	0·040	0	
	0·025	0·005	
0	0·020		
0·020	0·030		
0·045	0·040	0	0·25
	0·055	0	
	0·050	0·020	
0·020	0·030		
0·055	0·060		
	0·060	0	0·37
	0·070	0·035	
0·020	0·025		
0·060	0·060		
	0·080	0·020	0·50
	0·090	0·045	

TABLE 9

Effect of Slipstream on Mean Downwash and Velocity at Tailplane

Contra-rotating Propellers

Mid-wing with flaps down Wing-body angle 0 deg Deep rear body $l = 3 \cdot 78\bar{c}$

(a) ε at $T_c = 0$

α	C_L Trim	Z_t/D	
		0·10	0·30
−5·7	0·203	2·30	2·20
−3·6	0·409	2·80	2·40
−1·5	0·612	3·80	3·00
+0·6	0·835	4·60	4·30
+2·7	1·037	5·40	4·90

(b) Z_W/D

α	Z_t/D	
	0·1	0·3
−3·6	0·706	0·906
−1·5	0·650	0·850
+0·6	0·598	0·798
+2·7	0·542	0·742

(c) Z/D

Z_t/D	
0·1	0·3
+0·284	0·484
0·171	0·377
+0·069	0·270
−0·038	0·162

(d) $\Delta\varepsilon$

α	C_L Trim	Z_t/D	
		0·1	0·3
−3·6	0·481	0·60	0·30
−1·5	0·698	0·70	0·50
+0·6	0·930	0·90	0·40
+2·7	1·168	1·15	0·80
−1·5	0·772	1·10	0·90
+0·6	1·013	1·50	0·80
+2·7	1·248	1·90	1·30
0·6	1·092	2·30	1·20
2·7	1·312	2·40	1·50
0·6	1·143	2·60	1·70
2·7	1·391	2·90	2·00

(e) b

Z_t/D		T_c
0·1	0·3	
0	0	
0	0	
0	0	0·12
0·020	0	
0	0	
0·005	0·015	0·25
0·030	0	
0·005	0·025	0·37
0·040	0·010	
0·010	0·020	
0·045	0·005	0·50

TABLE 10

Lift and Pitching-Moment Coefficients Without Tailplane, without Flaps. Deep Rear Body

Single Rotating Propellers

(a) Low wing
Wing-body angle 0 deg
$l = 3 \cdot 78\bar{c}$

α (deg)	T_c	C_L	C_L Trim	C_m
−1·3	0	−0·024	−0·036	−0·0464
	0·37	−0·057	−0·072	−0·0574
	0·50	−0·064	−0·080	−0·0626
+0·25	0	+0·115	+0·109	−0·0214
1·3	0	0·195	0·193	−0·0059
	0·37	0·229	0·224	−0·0172
	0·5	0·235	0·229	−0·0222
2·35	0	0·293	0·295	+0·0091
3·4	0	0·380	0·385	0·0202
	0·37	0·472	0·474	0·0074
	0·5	0·497	0·498	0·0021
4·45	0	0·482	0·490	0·0307
5·5	0	0·581	0·592	0·0404
	0·37	0·723	0·730	0·0246
	0·5	0·758	0·763	0·0182
6·55	0	0·675	0·688	0·0493
7·55	0	0·767	0·782	0·0581
	0·37	0·965	+0·976	0·0422
	0·5	1·015	−1·024	0·0340
+8·6	0	+0·846	+0·865	+0·0704

(b) Low wing
Wing-body angle 0 deg
$l = 4 \cdot 41\bar{c}$

α (deg)	T_c	C_L	C_L Trim	C_m
−1·3	0	−0·020	−0·030	−0·0437
	0·37	−0·052	−0·065	−0·0563
	0·5	−0·060	−0·074	−0·0623
+0·25	0	+0·111	+0·106	−0·0214
1·3	0	0·201	0·199	−0·0075
	0·37	0·234	0·229	−0·0210
	0·5	0·247	0·241	−0·0268
2·35	0	0·288	0·290	+0·0083
3·4	0	0·382	0·386	+0·0194
	0·37	0·471	0·472	+0·0029
	0·5	0·494	0·493	−0·0028
4·45	0	0·475	0·482	+0·0310
5·5	0	0·577	0·586	0·0382
	0·37	0·723	0·728	0·0219
	0·5	0·759	0·762	0·0130
6·55	0	0·673	0·684	0·0465
7·55	0	0·765	0·778	0·0588
	0·37	0·957	0·966	0·0394
	0·5	1·008	1·015	0·0306
+8·6	0	+0·849	+0·866	+0·0730

Note : C_L includes component of propeller thrust
C_m excludes the moment of the thrust

TABLE 11

Effect of Slipstream on Mean Downwash and Velocity at Tailplane

Single Rotating Propellers

Low wing — Wing-body angle 0 deg — $l = 3{\cdot}78\bar{c}$

(a) ε deg at $T_c = 0$

α (deg)	C_L Trim	Z_t/D			
		0·16	0·31	0·46	0·61
−1·3	−0·036	0·55	−0·55	0·65	1·4
+0·25	+0·109	0·8	−0·05	1·2	1·8
1·3	0·193	1·1	+0·25	1·5	2·15
2·35	0·295	1·45	0·65	1·85	2·55
3·4	0·385	1·85	1·05	2·25	2·75
4·45	0·490	2·45	1·3	2·55	3·25
5·5	0·592	2·95	1·6	3·0	3·45
6·55	0·688	3·45	2·15	3·6	3·9
7·55	0·782	4·0	2·4	3·9	4·45
+8·6	+0·865	3·8	+2·5	4·15	4·95

(b) Z_W/D

α (deg)	Z_t/D			
	0·16	0·31	0·46	0·61
−1·3	0·219	0·369	0·519	0·669
+1·3	0·138	0·288	0·438	0·588
3·4	0·075	0·224	0·374	0·524
5·5	0·014	0·164	0·313	0·462
+7·55	−0·047	0·102	0·251	0·399

(c) $\dfrac{Z_W/D}{l/\bar{c}}$

α (deg)	Z_t/D			
	0·16	0·31	0·46	0·61
−1·3	+0·058	0·098	0·137	0·177
+1·3	0·037	0·076	0·116	0·156
3·4	0·020	0·059	0·099	0·139
5·5	+0·004	0·043	0·083	0·122
+7·55	−0·012	0·027	0·066	0·106

TABLE 11—*continued*

(d) $\Delta\varepsilon$ deg

α (deg)	C_L Trim	Z_t/D 0·16	0·31	0·46	0·61	T_c
−1·3	−0·072	1·45	1·0	0·3	0·2	
+1·3	+0·224	1·45	1·45	0·95	0·45	
3·4	0·474	0·95	1·55	1·5	0·95	0·37
5·5	0·730	0·5	1·7	1·95	1·6	
+7·55	+0·976	0·1	1·3	1·95	1·8	
−1·3	−0·080	2·0	1·45	0·65	0·4	
+1·3	−0·229	1·65	1·9	1·4	0·85	
3·4	−0·498	1·15	2·0	2·1	1·55	0·5
5·5	−0·763	0·6	2·2	2·55	2·25	
+7·55	−1·024	0·25	1·85	2·6	2·45	

(e) $\Delta\varepsilon$ deg $\frac{l}{\bar{c}}$

α (deg)	C_L Trim	Z_t/D 0·16	0·31	0·46	0·61	T_c
−1·3	−0·072	5·48	3·78	1·13	0·76	
+1·3	+0·224	5·48	5·48	3·59	1·71	
3·4	0·474	3·59	5·86	5·67	3·59	0·37
5·5	0·730	1·89	6·43	7·37	6·05	
+7·55	+0·976	0·38	4·91	7·37	6·81	
−1·3	−0·080	7·56	5·48	2·46	1·51	
+1·3	−0·229	6·24	7·18	5·29	3·21	
3·4	−0·498	4·35	7·56	7·94	5·86	0·5
5·5	−0·763	2·27	8·32	9·65	8·51	
+7·55	−1·024	0·94	7·00	9·83	9·26	

(f) b

α (deg)	C_L Trim	Z_t/D 0·16	0·31	0·46	0·61	T_c
−1·3	−0·072	0·104	0·029	0·010	0·0	
+1·3	+0·224	0·189	0·074	0·005	0·0	
3·4	0·474	0·271	0·162	0·054	0·013	0·37
5·5	0·730	0·229	0·227	0·148	0·044	
+7·55	+0·976	0·194	0·261	0·185	0·093	
−1·3	−0·080	0·125	0·052	0·013	0·001	
+1·3	−0·229	0·225	0·112	0·022	0·010	
3·4	−0·498	0·326	0·217	0·090	0·046	0·5
5·5	−0·763	0·314	0·284	0·198	0·069	
+7·55	−1·024	0·292	0·329	0·232	0·117	

TABLE 12

Effect of Slipstream on Mean Downwash and Velocity at Tailplane

Single Rotating Propellers

Low wing — Wing-body angle 0 deg — $l = 4{\cdot}41\bar{c}$

(a) ε deg at $T_c = 0$

α (deg)	C_L Trim	Z_t/D	
		0·46	0·61
−1·3	−0·030	0·15	0·9
+0·25	+0·106	0·8	1·5
1·3	0·199	1·2	1·9
2·35	0·290	1·65	2·45
3·4	0·386	2·05	2·80
4·45	0·482	2·55	3·15
5·5	0·586	3·15	3·6
6·55	0·684	3·6	4·35
7·55	0·718	3·8	4·8
+8·6	+0·866	4·2	5·4

(b) Z_W/D

α (deg)	Z_t/D	
	0·46	0·61
−1·3	0·534	0·684
+1·3	0·435	0·585
3·4	0·354	0·504
5·5	0·278	0·427
+7·55	0·203	0·351

(c) $\dfrac{Z_W/D}{l/\bar{c}}$

α (deg)	Z_t/D	
	0·46	0·61
−1·3	0·121	0·155
+1·3	0·099	0·133
3·4	0·080	0·114
5·5	0·063	0·097
+7·55	0·046	0·080

(d) $\Delta\varepsilon$ deg

α (deg)	C_L Trim	Z_t/D		T_c
		0·46	0·61	
−1·3	−0·065	0·45	0·25	0·37
+1·3	+0·229	1·1	0·65	
3·4	0·472	1·65	1·0	
5·5	0·728	1·6	1·6	
+7·55	+0·996	1·65	1·6	
−1·3	−0·074	0·7	0·4	0·5
+1·3	+0·241	1·5	0·9	
3·4	0·493	2·2	1·4	
5·5	0·762	2·15	2·15	
+7·55	+1·015	2·15	2·2	

(e) $\Delta\varepsilon$ deg $\times \dfrac{l}{\bar{c}}$

α (deg)	C_L Trim	Z_t/D		T_c
		0·46	0·61	
−1·3	−0·065	1·98	1·10	0·37
+1·3	+0·229	4·85	2·87	
3·4	0·472	7·28	4·41	
5·5	0·728	7·06	7·06	
+7·55	+0·966	7·28	7·06	
−1·3	−0·074	3·09	1·76	0·5
+1·3	+0·247	6·62	3·97	
3·4	0·493	9·70	6·18	
5·5	0·762	9·48	9·48	
+7·55	+1·015	9·48	9·70	

(f) b

α (deg)	C_L Trim	Z_t/D		T_c
		0·46	0·61	
−1·3	−0·065	0	0	0·37
+1·3	+0·229	0·011	0·006	
3·4	0·472	0·063	0·020	
5·5	0·728	0·152	0·077	
7·55	+0·966	0·245	0·113	
−1·3	−0·074	0	0	0·5
+1·3	+0·247	0·032	0·006	
3·4	0·493	0·100	0·057	
5·5	0·762	0·210	0·118	
+7·55	+1·015	0·304	0·183	

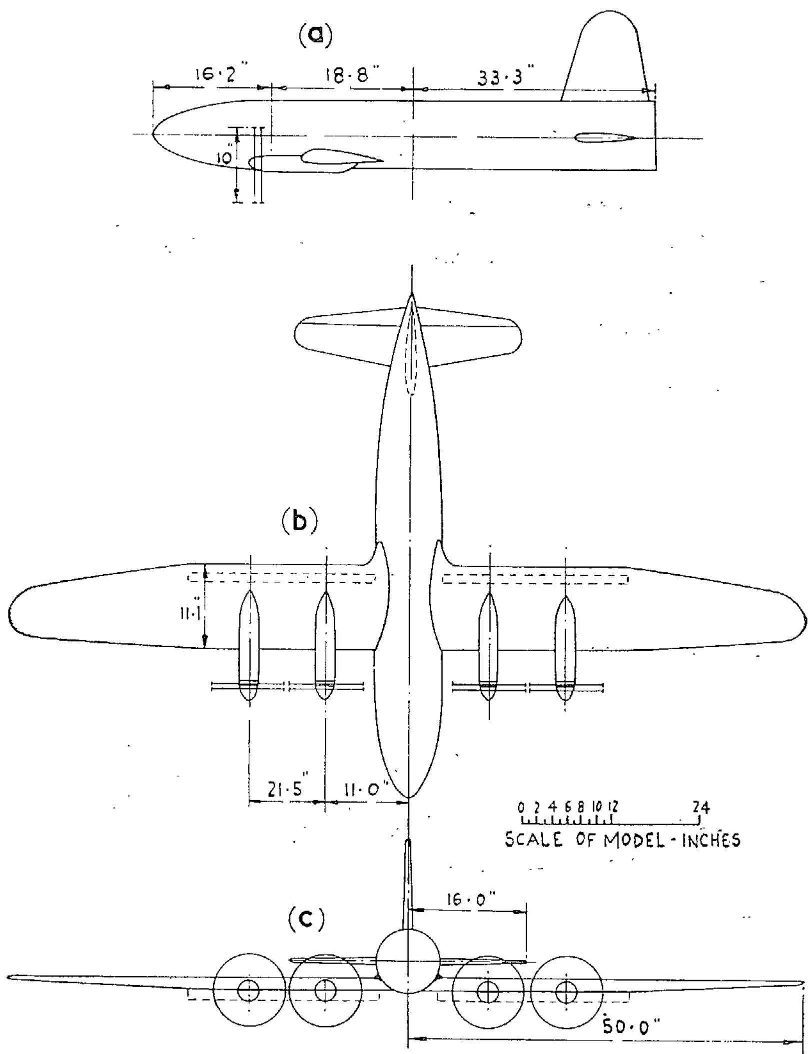

FIG. 1. General arrangement of model, with low wing, 0-deg wing-body angle, tail arm (i).

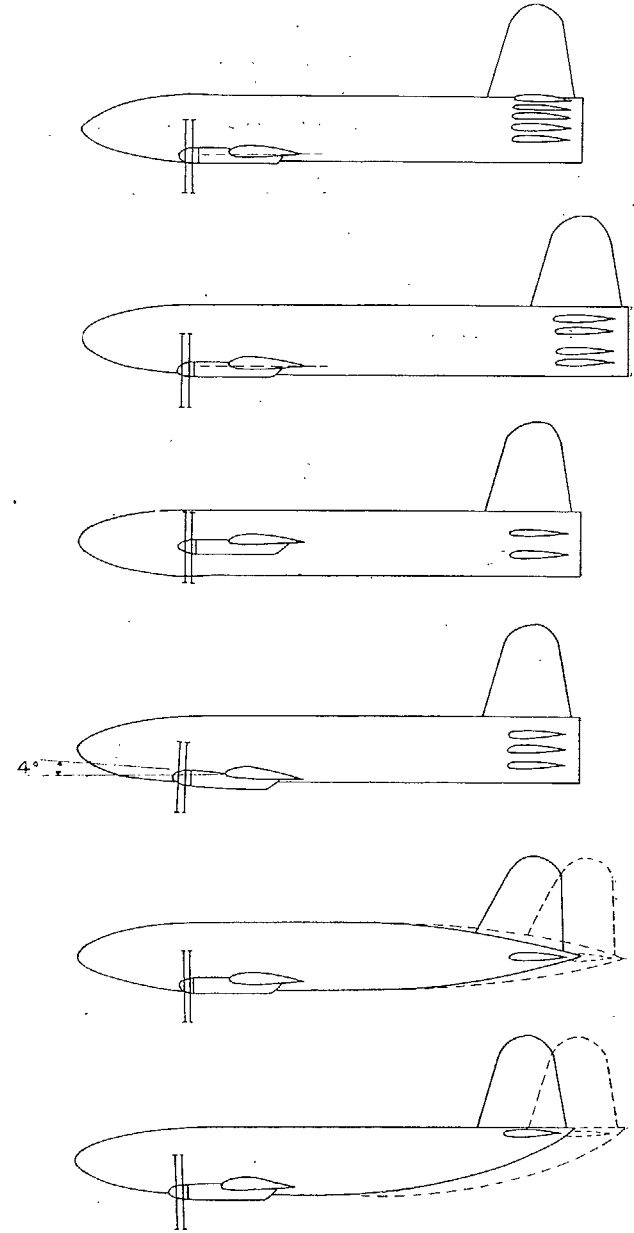

FIG. 2. Wing-body arrangements and tailplane heights. Flaps up.

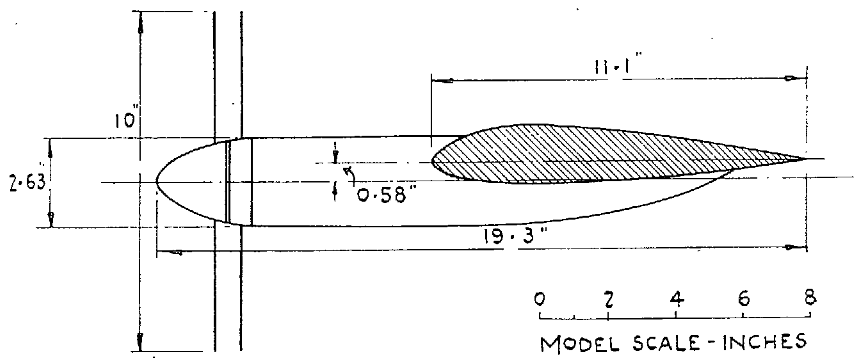

FIG. 3. Detail of nacelle.

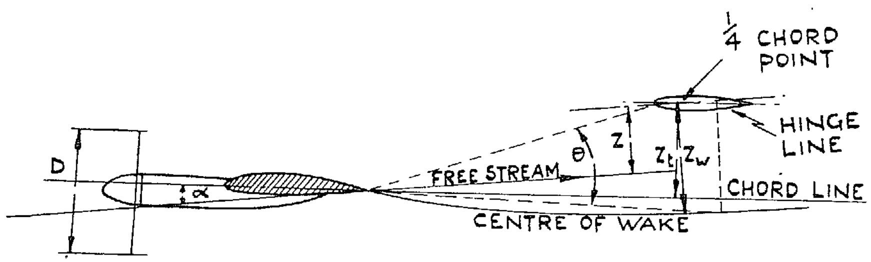

FIG. 4. Notation.

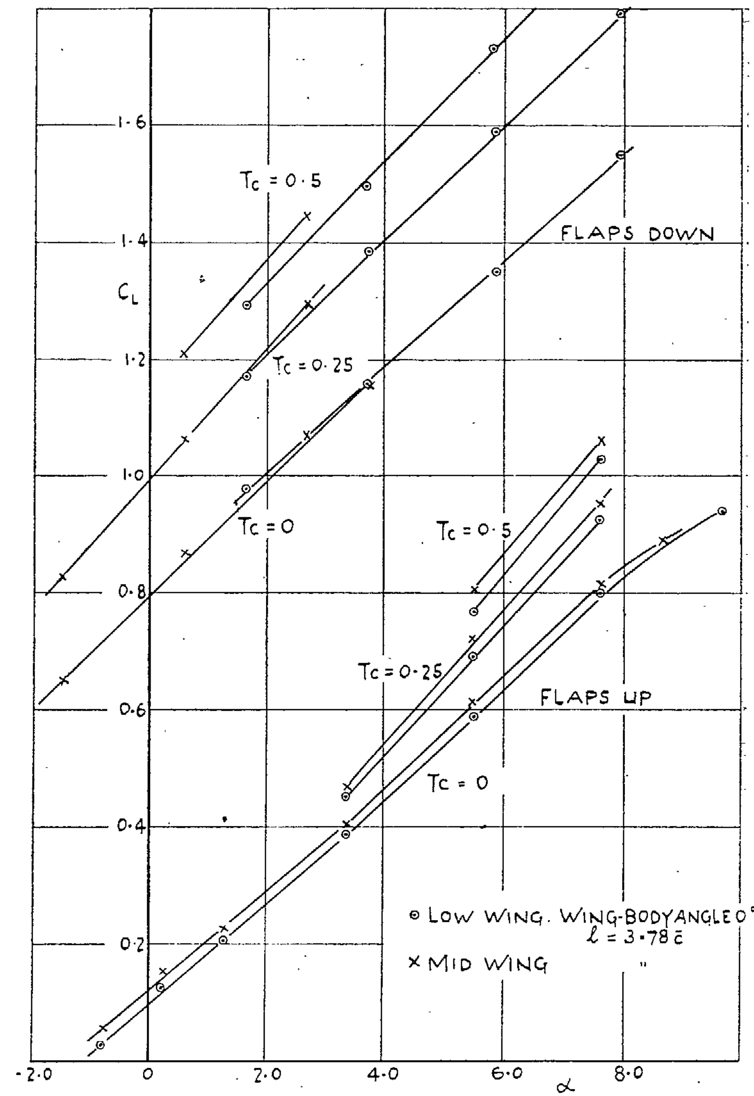

FIG. 5. Lift coefficients without tailplane for two wing-body arrangements.
Contra-rotating propellers.

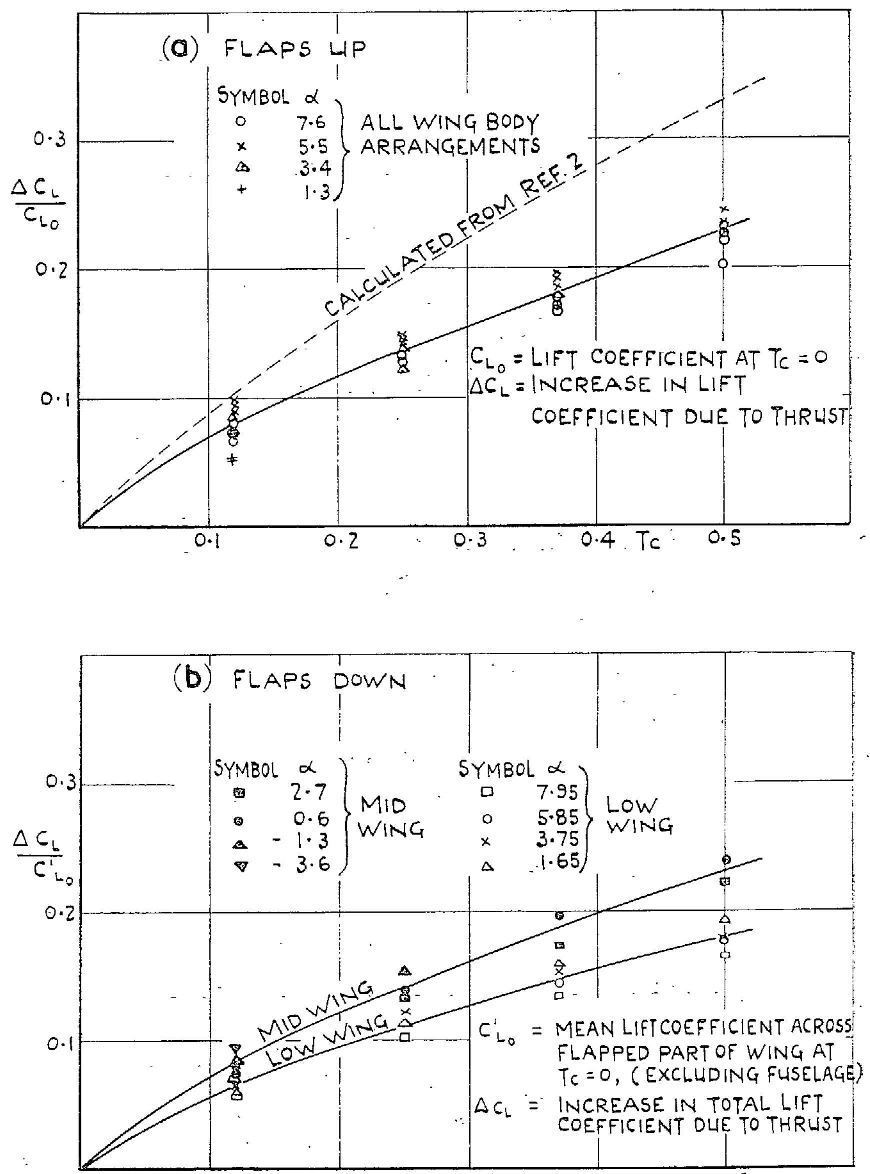

FIG. 7. Fractional increase in lift due to slipstream. Contra-rotating propellers.

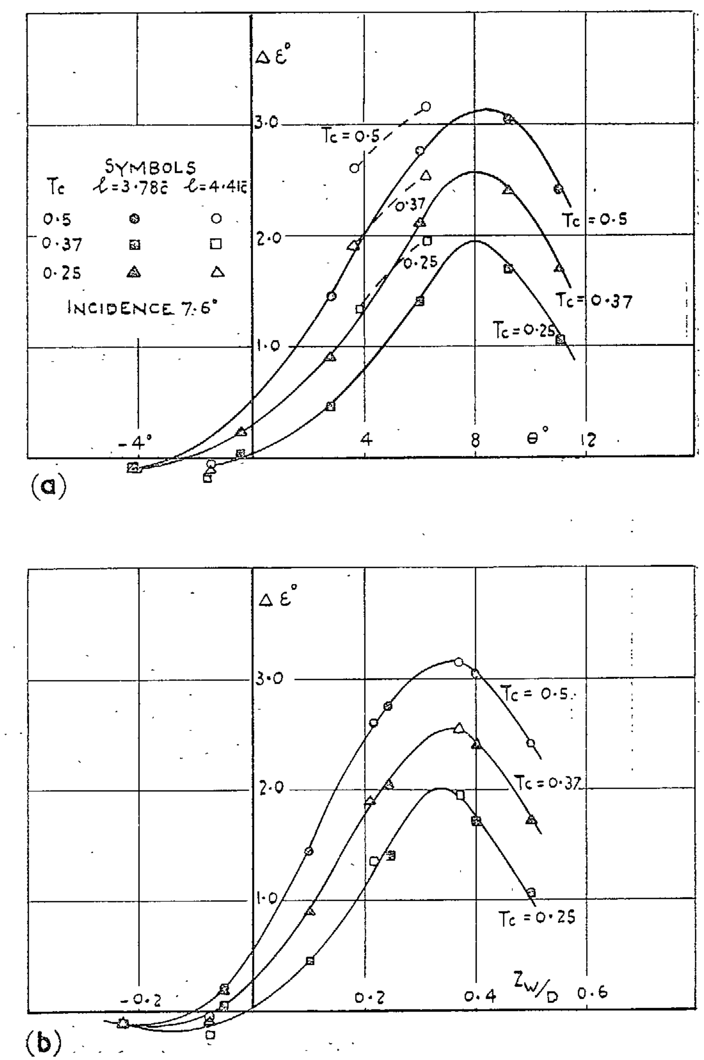

FIG. 8. Downwash increments for two tail arms. Contra-rotating propellers.

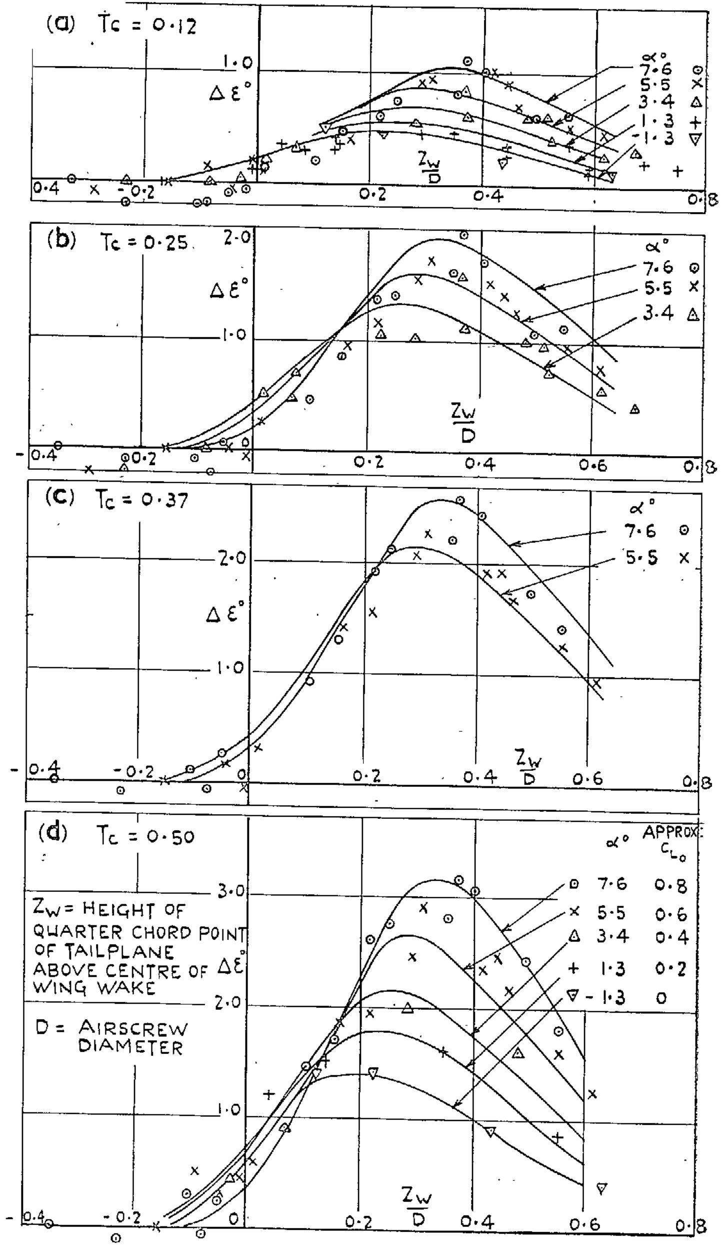

FIG. 9. Increment of downwash at tailplane against tailplane height above centre of wake. Flaps up. Contra-rotating propellers.

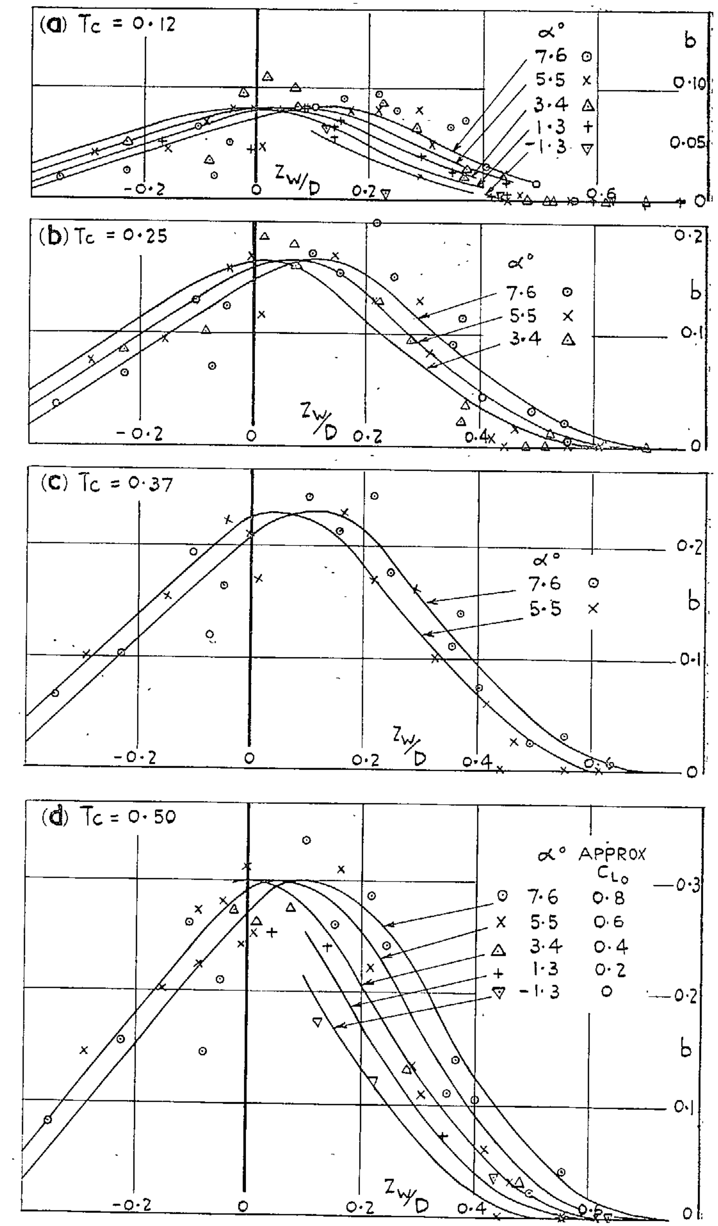

FIG. 10. Increment of velocity at tailplane against tailplane height above centre of wake. Flaps up. Contra-rotating propellers.

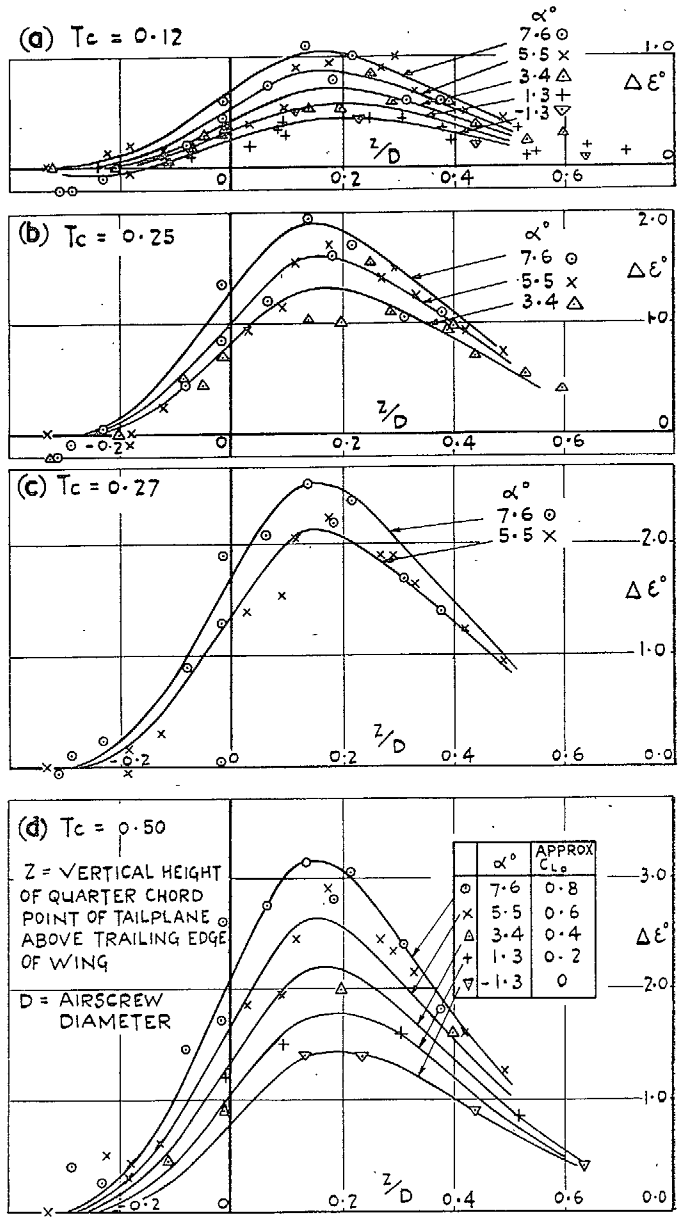

FIG. 11. Increment of downwash at tailplane against tailplane height from trailing edge of wing. Flaps up. Contra-rotating propellers.

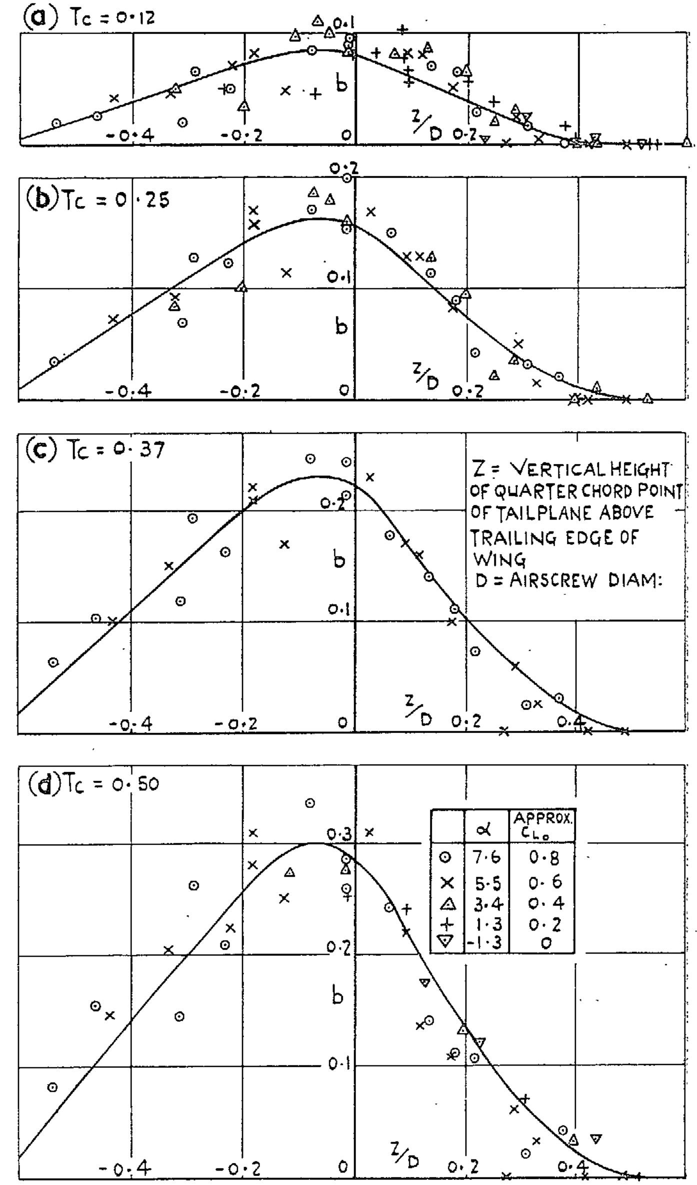

FIG. 12. Increment of velocity at tailplane against tailplane height from trailing edge of wing. Flaps up. Contra-rotating propellers.

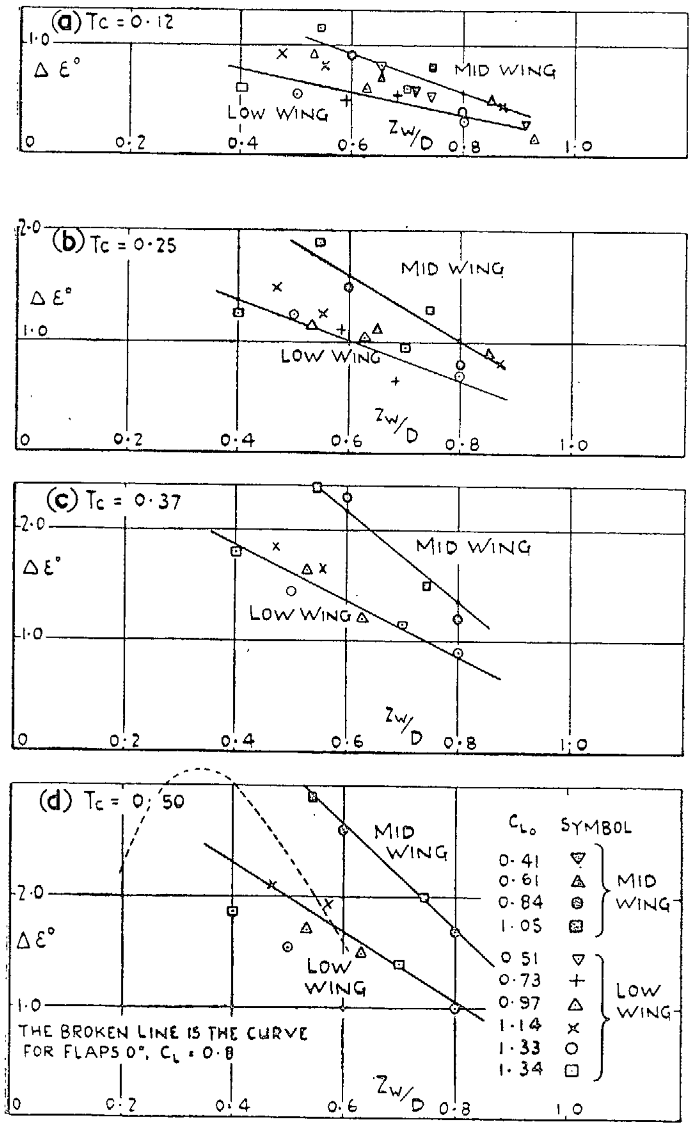

FIG. 13. Increment of downwash at tailplane against tailplane height above centre of wake. Flaps down. Contra-rotating propellers.

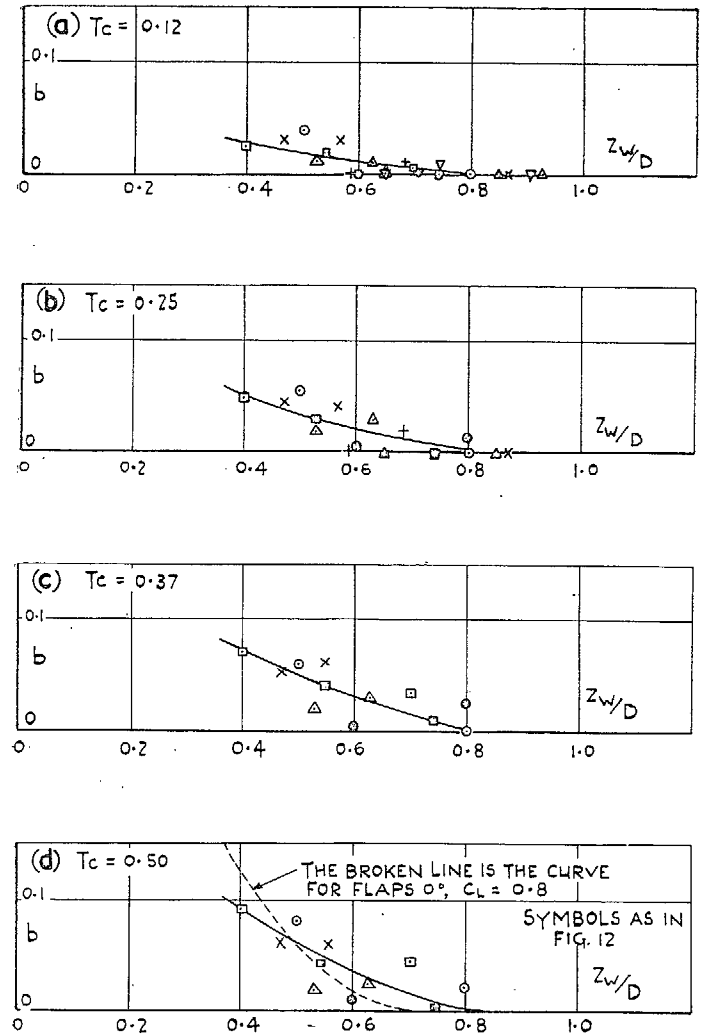

FIG. 14. Increment of velocity at tailplane against tailplane height above centre of wake. Flaps down. Contra-rotating propellers.

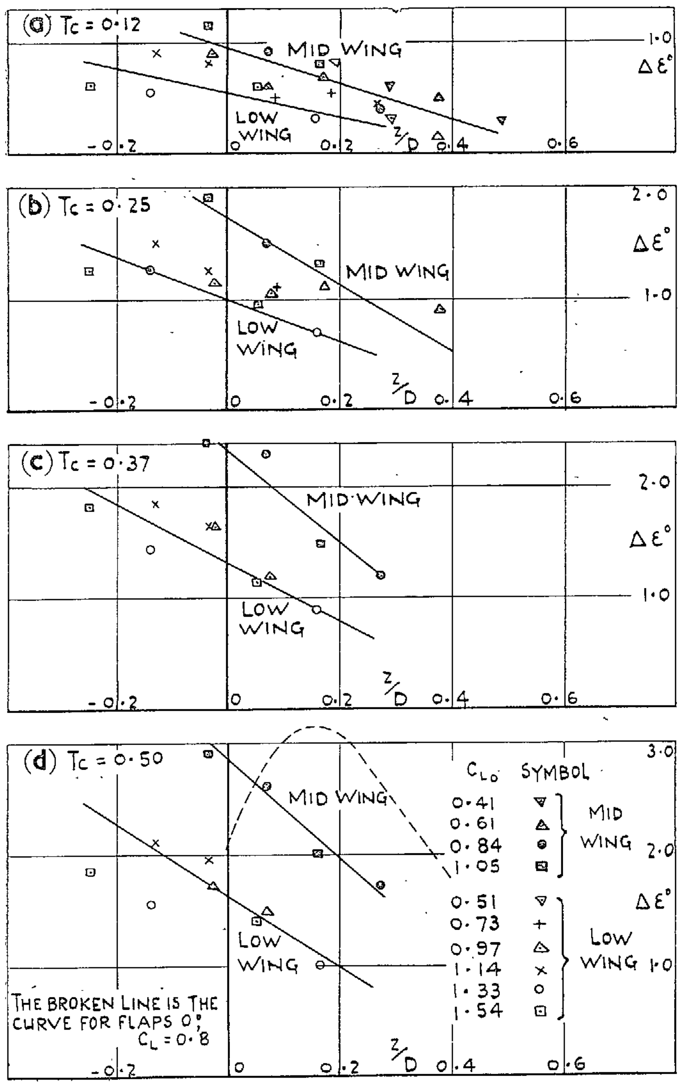

FIG. 15. Increment of downwash at tailplane against tailplane height from trailing edge of wing. Flaps down. Contra-rotating propellers.

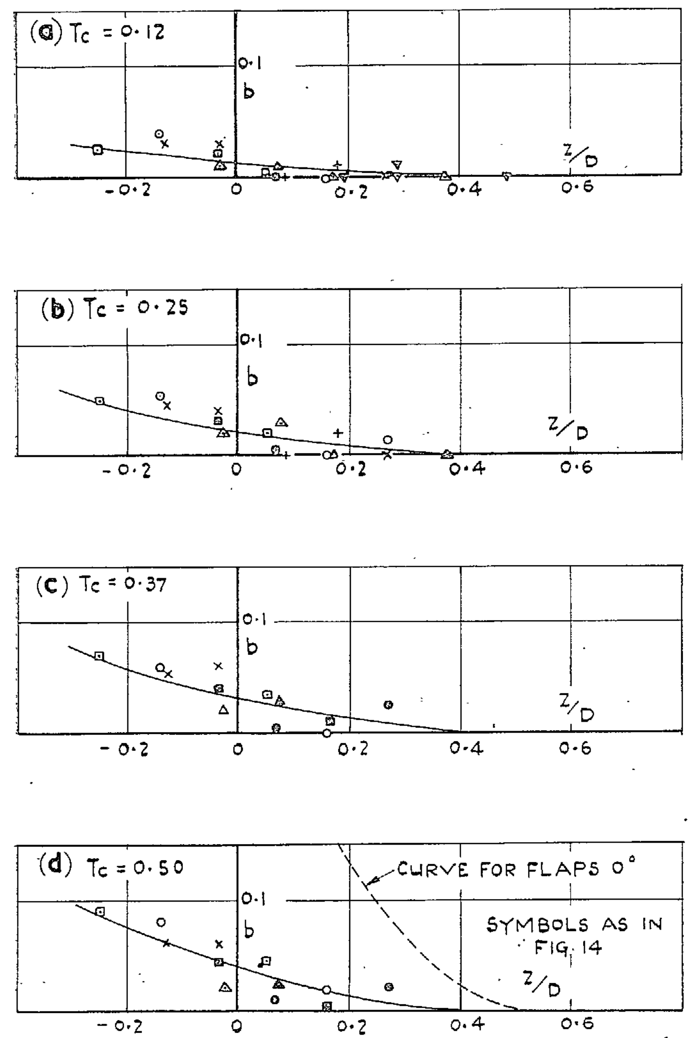

FIG. 16. Increment of velocity at tailplane against tailplane height from trailing edge of wing. Flaps down. Contra-rotating propellers.

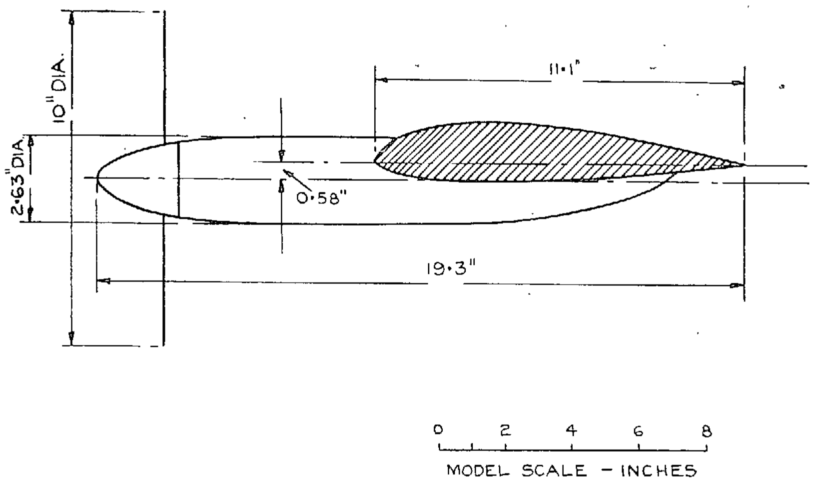

FIG. 17. Detail of nacelle.

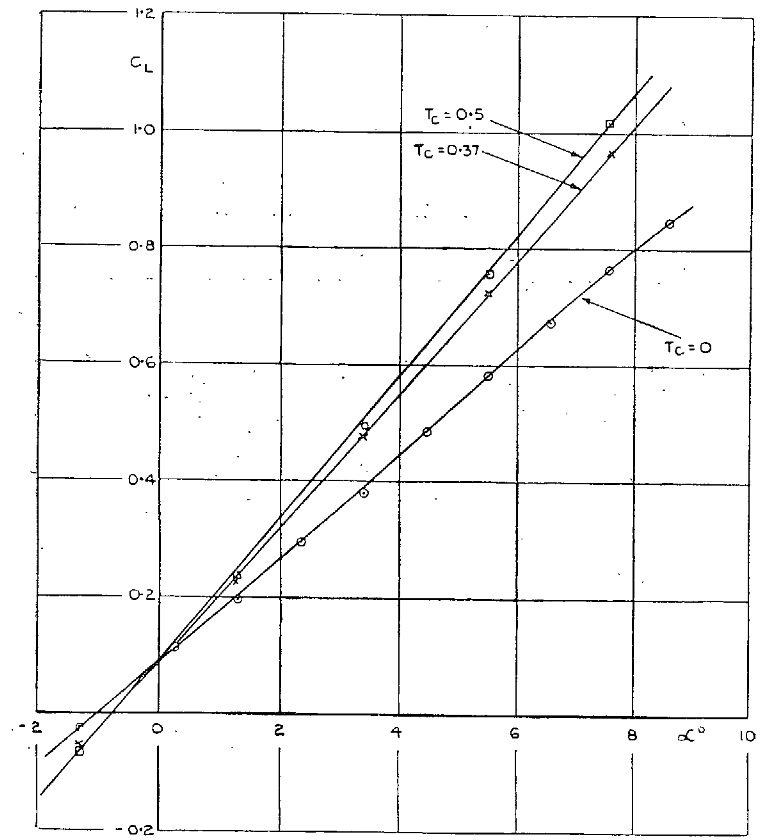

FIG. 18. Lift coefficients without tailplane. Low wing, wing-body angle 0 deg. $l = 3{\cdot}78\bar{c}$. Single rotating propellers.

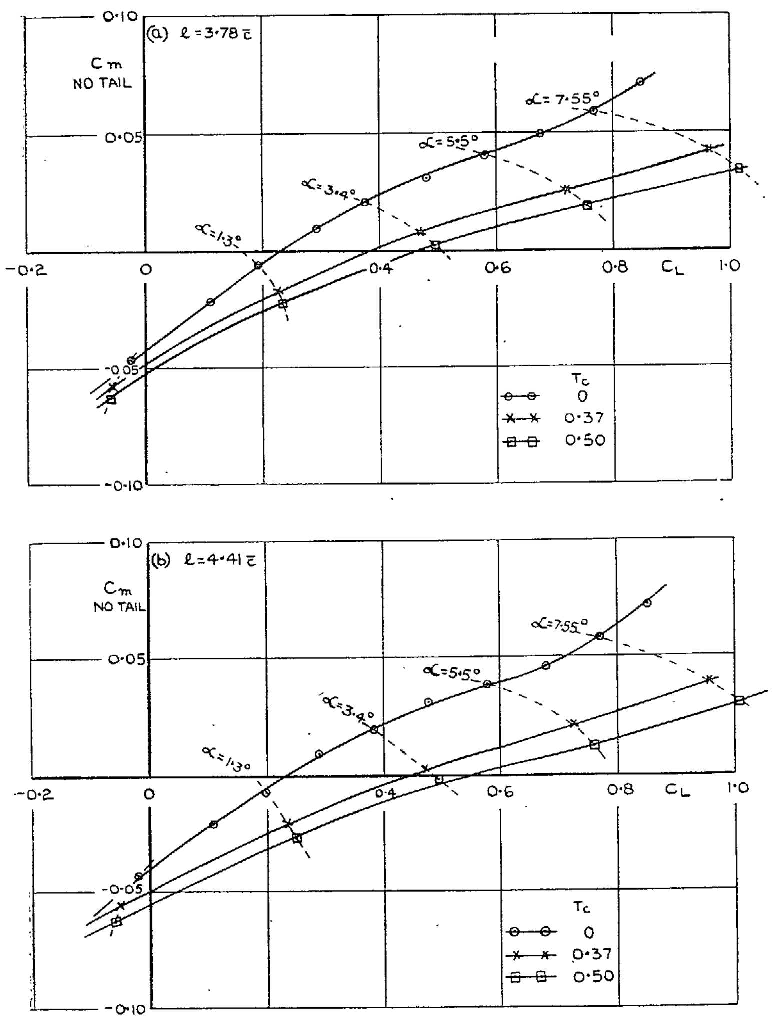

FIG. 19. Pitching-moment coefficients without tailplane. Low wing, wing-body angle 0 deg. Single rotating propellers.

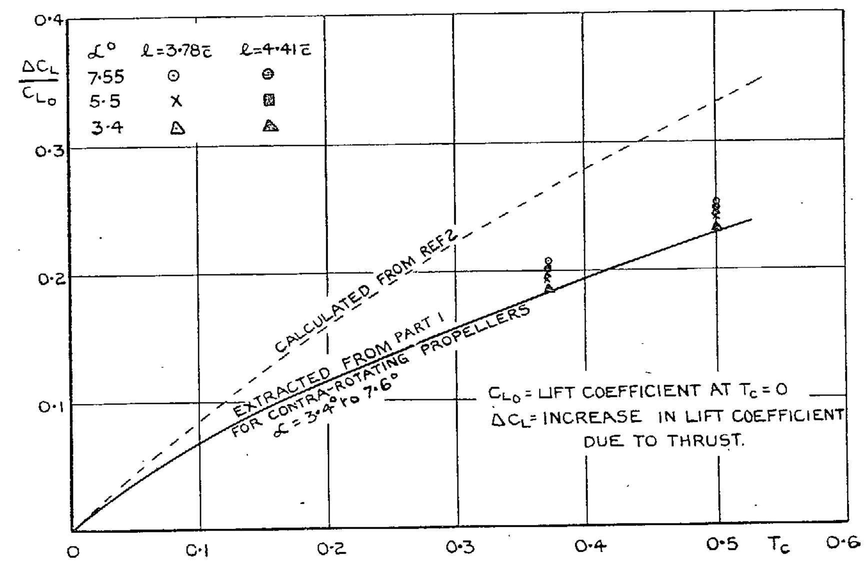

FIG. 20. Fractional increase in lift due to slipstream. Single rotating propellers.

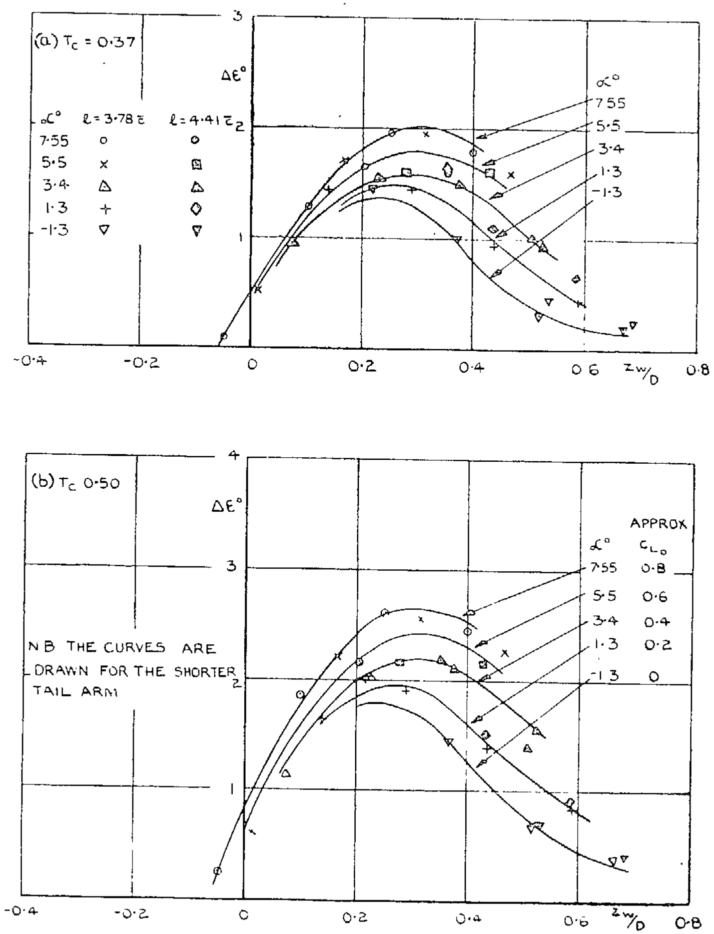

FIG. 21. Increment of downwash at tailplane against tailplane height above centre of wake.
Single rotating propellers.

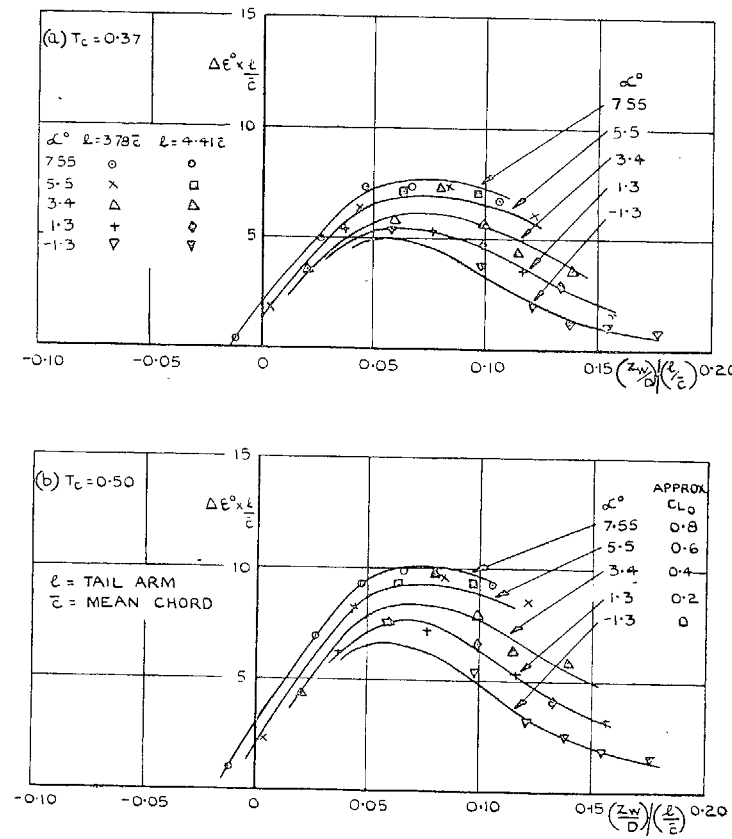

FIG. 22. Increments of downwash at tailplane.
Effect of tail arm.
Single rotating propellers.

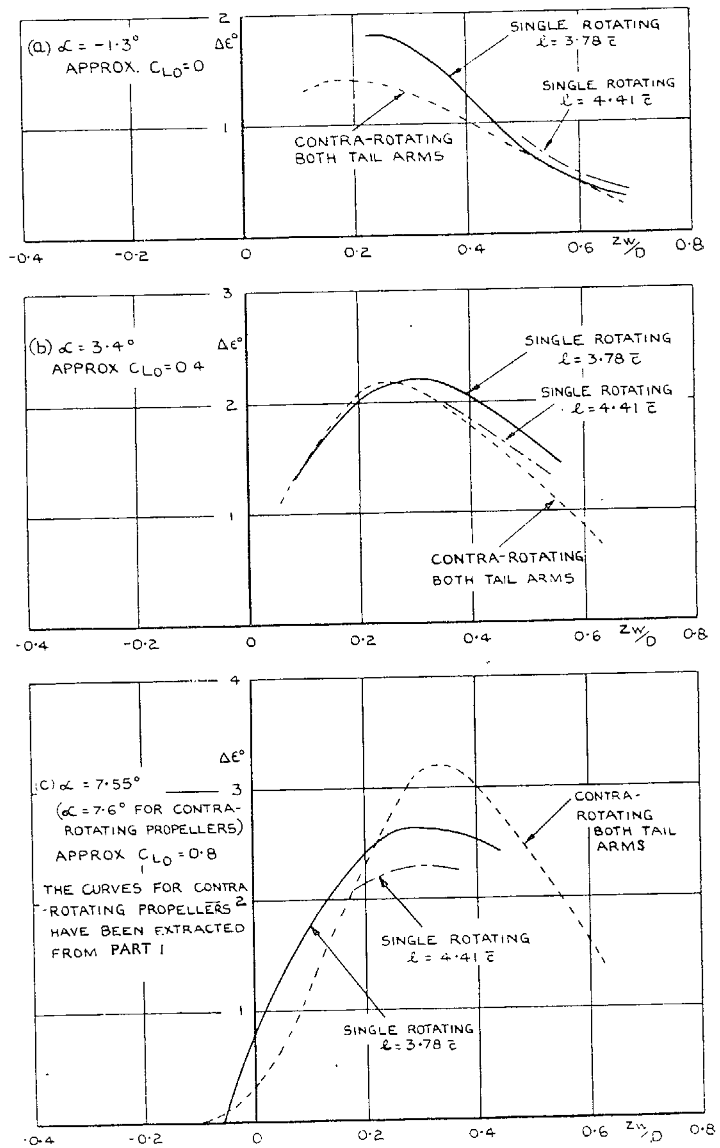

FIG. 23. Comparison of downwash increments for single and contra-rotating propellers. $T_c = 0 \cdot 5$.

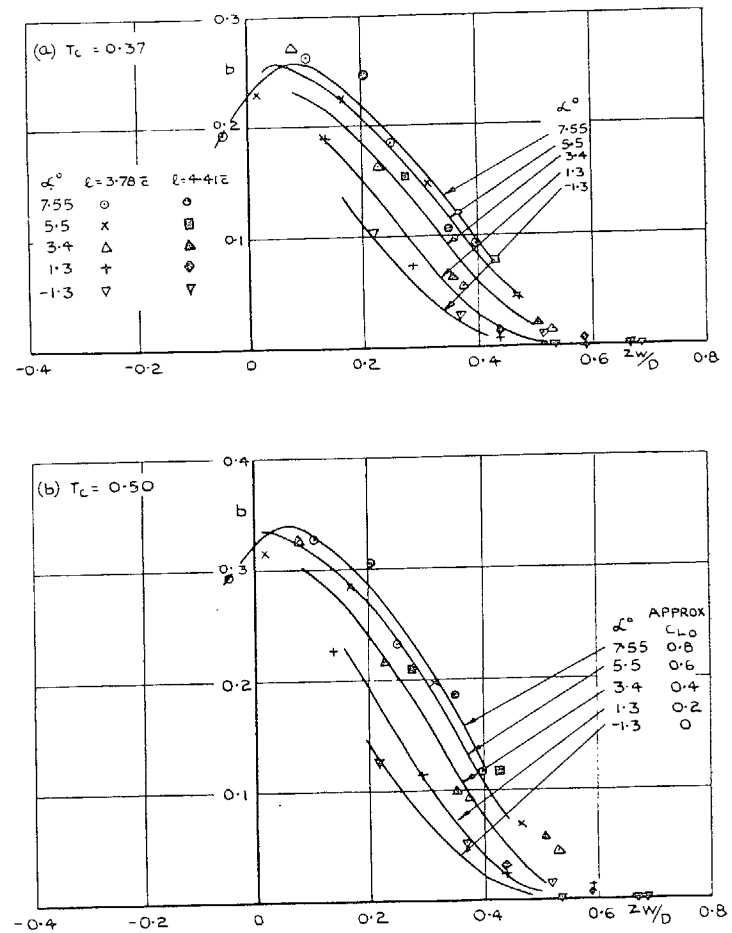

FIG. 24. Increment of velocity at tailplane against tailplane height above centre of wake. Single rotating propellers.

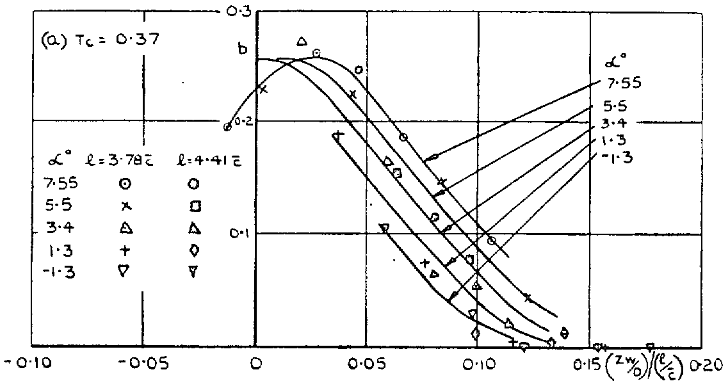

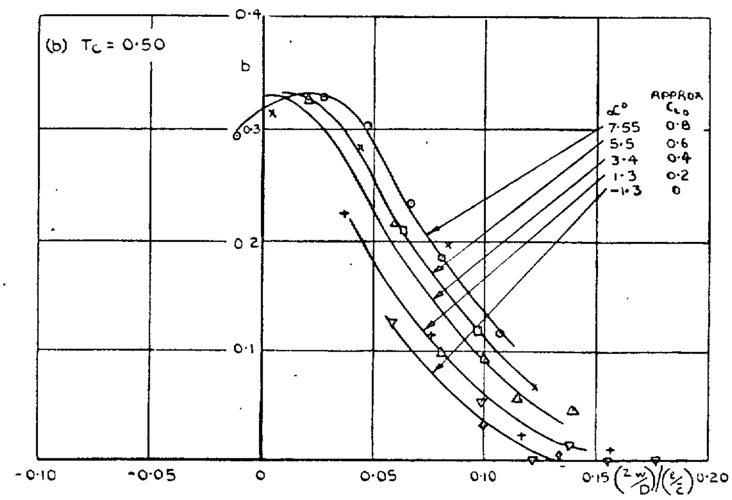

FIG. 25. Increment of velocity at tailplane. Effect of tail arm. Single rotating propellers.

J4312 Wt.18/9296 K9 6/55 D&Co. 34/263 PRINTED IN GREAT BRITAIN

C

Publications of the Aeronautical Research Council

ANNUAL TECHNICAL REPORTS OF THE AERONAUTICAL RESEARCH COUNCIL (BOUND VOLUMES)

1936 Vol. I. Aerodynamics General, Performance, Airscrews, Flutter and Spinning. 40s. (41s. 1d).
Vol. II. Stability and Control, Structures, Seaplanes, Engines, etc. 50s. (51s. 1d.)
1937 Vol. I. Aerodynamics General, Performance, Airscrews, Flutter and Spinning. 40s. (41s. 1d.)
Vol. II. Stability and Control, Structures, Seaplanes, Engines, etc. 60s. (61s. 1d.)
1938 Vol. I. Aerodynamics General, Performance, Airscrews. 50s. (51s. 1d.)
Vol. II. Stability and Control, Flutter, Structures, Seaplanes, Wind Tunnels, Materials. 30s. (31s. 1d.)
1939 Vol. I. Aerodynamics General, Performance, Airscrews, Engines. 50s. (51s. 1d.)
Vol. II. Stability and Control, Flutter and Vibration, Instruments, Structures, Seaplanes, etc. 63s. (64s. 2d.)
1940 Aero and Hydrodynamics, Aerofoils, Airscrews, Engines, Flutter, Icing, Stability and Control, Structures, and a miscellaneous section. 50s. (51s. 1d.)
1941 Aero and Hydrodynamics, Aerofoils, Airscrews, Engines, Flutter, Stability and Control, Structures. 63s. (64s. 2d.)
1942 Vol. I. Aero and Hydrodynamics, Aerofoils, Airscrews, Engines. 75s. (76s. 3d.)
Vol. II. Noise, Parachutes, Stability and Control, Structures, Vibration, Wind Tunnels. 47s. 6d. (48s. 7d.)
1943 Vol. I. Aerodynamics, Aerofoils, Airscrews, 80s. (81s. 4d.)
Vol. II. Engines, Flutter, Materials, Parachutes, Performance, Stability and Control, Structures. 90s. (91s. 6d.)
1944 Vol. I. Aero and Hydrodynamics, Aerofoils, Aircraft, Airscrews, Controls. 84s. (85s. 8d.)
Vol. II. Flutter and Vibration, Materials, Miscellaneous, Navigation, Parachutes, Performance, Plates, and Panels, Stability, Structures, Test Equipment, Wind Tunnels. 84s. (85s. 8d.)

ANNUAL REPORTS OF THE AERONAUTICAL RESEARCH COUNCIL—

1933–34	1s. 6d. (1s. 8d.)	1937	2s. (2s. 2d.)
1934–35	1s. 6d. (1s. 8d.)	1938	1s. 6d. (1s. 8d.)
April 1, 1935 to Dec. 31, 1936.	4s. (4s. 4d.)	1939–48	3s. (3s. 2d.)

INDEX TO ALL REPORTS AND MEMORANDA PUBLISHED IN THE ANNUAL TECHNICAL REPORTS, AND SEPARATELY—

April, 1950 - - - - - R. & M. No. 2600. 2s. 6d. (2s. 7½d.)

AUTHOR INDEX TO ALL REPORTS AND MEMORANDA OF THE AERONAUTICAL RESEARCH COUNCIL—

1909–1949 - - - - - - R. & M. No. 2570. 15s. (15s. 3d.)

INDEXES TO THE TECHNICAL REPORTS OF THE AERONAUTICAL RESEARCH COUNCIL—

December 1, 1936 — June 30, 1939.	R. & M. No. 1850.	1s. 3d. (1s. 4½d.)
July 1, 1939 — June 30, 1945.	R. & M. No. 1950.	1s. (1s. 1½d.)
July 1, 1945 — June 30, 1946.	R. & M. No. 2050.	1s. (1s. 1½d.)
July 1, 1946 — December 31, 1946.	R. & M. No. 2150.	1s. 3d. (1s. 4½d.)
January 1, 1947 — June 30, 1947.	R. & M. No. 2250.	1s. 3d. (1s. 4½d.)
July, 1951 - - - -	R. & M. No. 2350.	1s. 9d. (1s. 10½d.)

Prices in brackets include postage.

Obtainable from

HER MAJESTY'S STATIONERY OFFICE

York House, Kingsway, London W.C.2 ; 423 Oxford Street, London W.1 (Post Orders : P.O. Box No. 569, London S.E.1) ; 13A Castle Street, Edinburgh 2 ; 39 King Street, Manchester 2 ; 2 Edmund Street, Birmingham 3 ; 109 St. Mary Street, Cardiff ; Tower Lane, Bristol 1 ; 80 Chichester Street, Belfast OR THROUGH ANY BOOKSELLER

S.O. Code No. 23-2747

R. & M. No. 2747